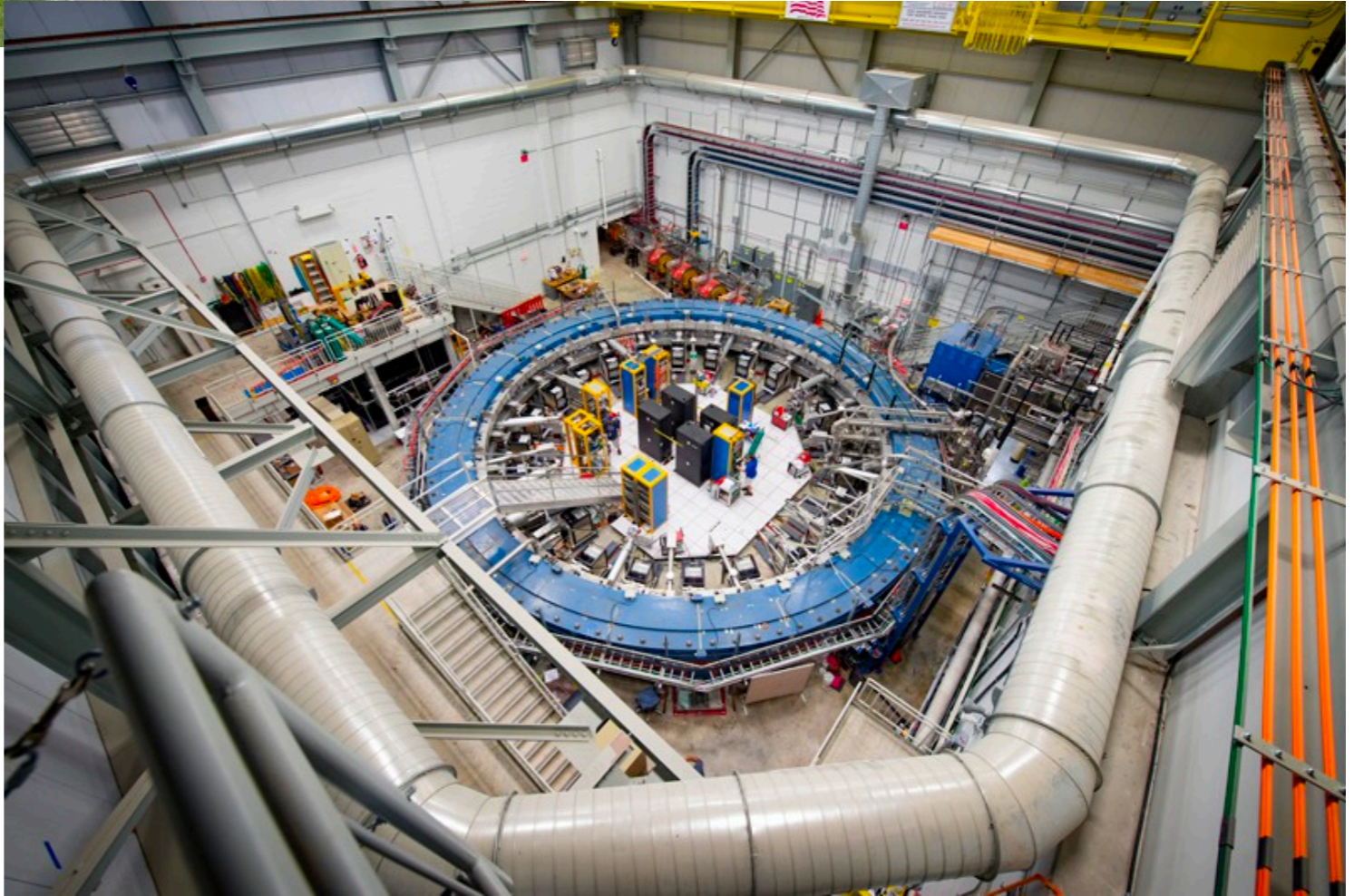
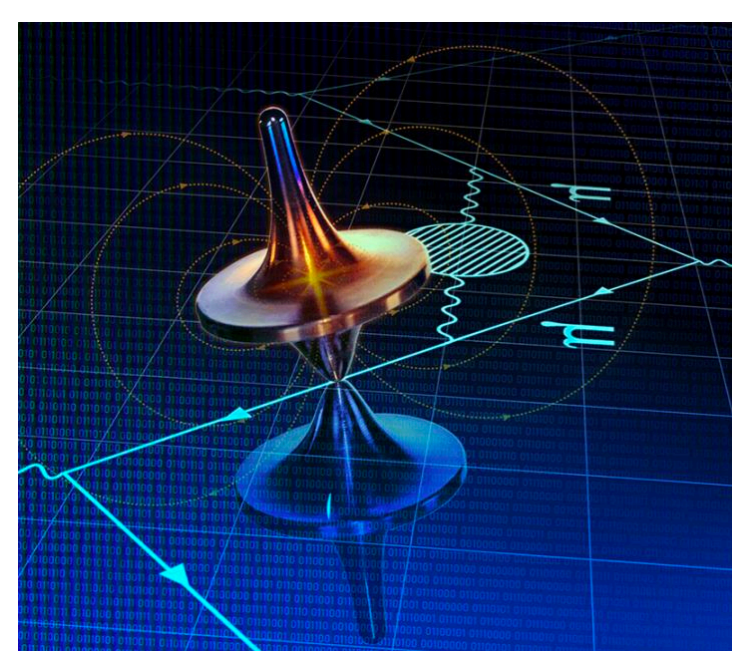


Новая физика, где она?



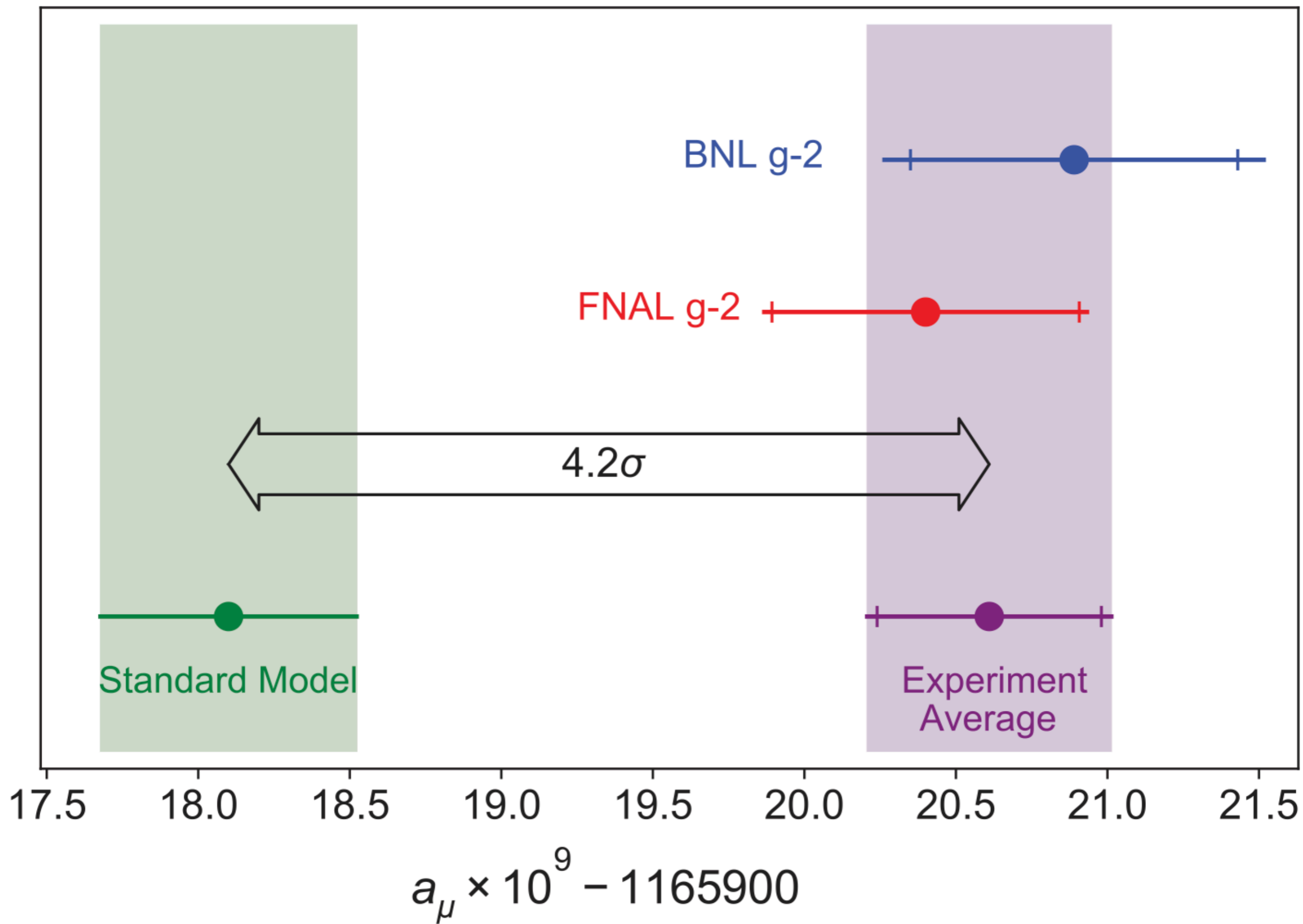


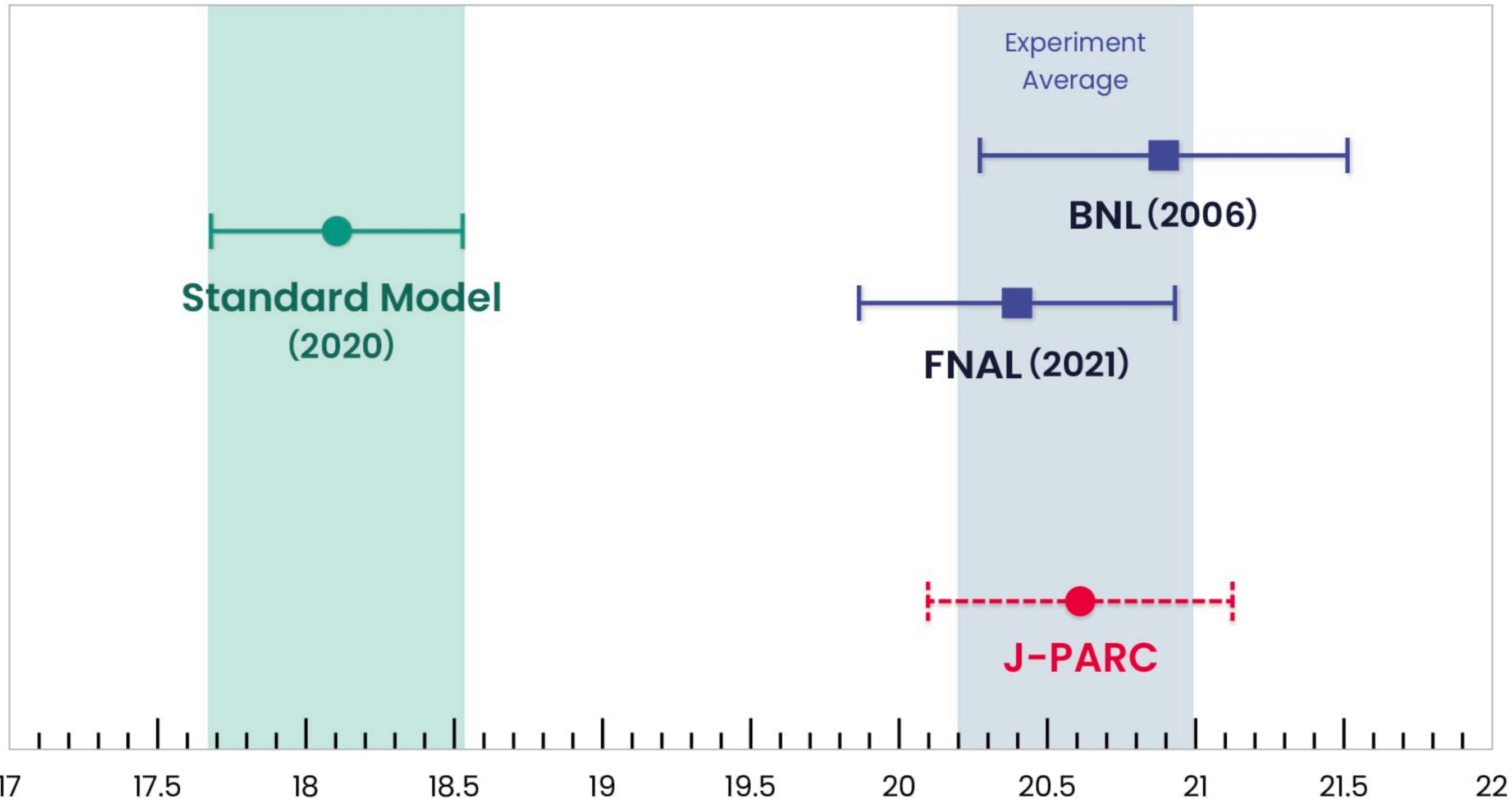
	Section	Equation	Value $\times 10^{11}$	References					
E821)		Eq. (8.13)	116 592 089(63)	Ref. [1]					
HVP LO (e^+e^-)	Sec. 2.3.7	Eq. (2.33)	6931(40)	Refs. [2–7]					
HVP NLO (e^+e^-)	Sec. 2.3.8	Eq. (2.34)	−98.3(7)	Ref. [7]					
HVP NNLO (e^+e^-)	Sec. 2.3.8	Eq. (2.35)	12.4(1)	Ref. [8]					
HVP LO (lattice, $udsc$)	Sec. 3.5.1	Eq. (3.49)	7116(184)	Refs. [9–17]					
HLbL (phenomenology)	Sec. 4.9.4	Eq. (4.92)	92(19)	Refs. [18–30]					
HLbL NLO (phenomenology)	Sec. 4.8	Eq. (4.91)	2(1)	Ref. [31]					
HLbL (lattice, uds)	Sec. 5.7	Eq. (5.49)	79(35)	Ref. [32]					
HLbL (phenomenology + lattice)	Sec. 8	Eq. (8.10)	90(17)	Refs. [18–30, 32]					
QED	Sec. 6.5	Eq. (6.30)	116 584 718.931(104)	Refs. [33, 34]					
Electroweak									
HVP (e^+e^- , LO + NLO + NNLO)									
HLbL (phenomenology + lattice)									
Total SM Value									
Difference: $\Delta a_\mu := a_\mu^{\text{exp}} - a_\mu^{\text{SM}}$									
	(1)	(2)	(3)	(4)	(5)	(6)	(7)	(8)	(9)
	(10)	(11)	(12)	(13)	(14)	(15)	(16)	(17)	(18)
	(19)	(20)	(21)	(22)	(23)	(24)	(25)		

Table 1: Summary of the contributions to a_μ from the Standard Model (SM) and the experimental value. The first block summarizes the contributions from Secs. 2 to 5 as well as the total HLbL number. The second block summarizes the quantities and the total HLbL number. The constraints are given in parentheses. The final rounding includes the uncertainty from the lattice QCD calculations [89]. In addition, the HLbL evaluation uses crucial methodological advances from measurements of the Cs atom [117].

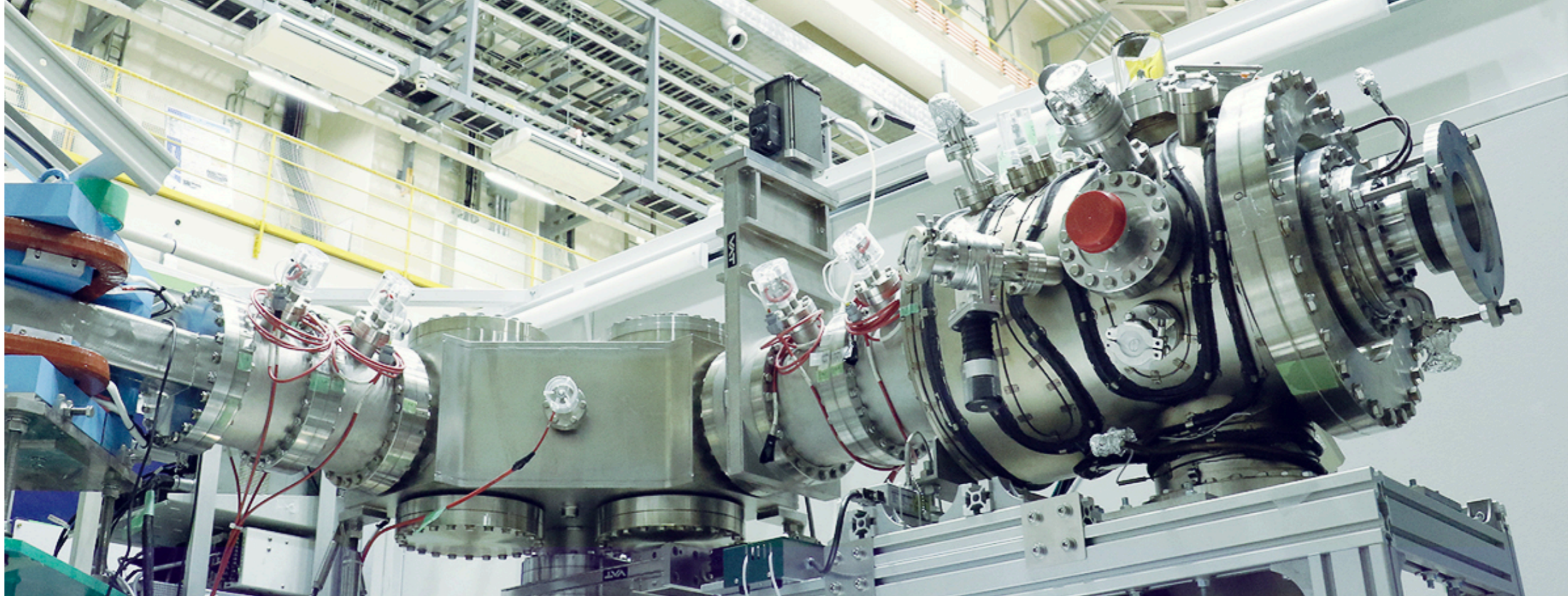
Contribution	Section	Equation	Value $\times 10^{11}$	References
Experiment (E821)		Eq. (8.13)	116 592 089(63)	Ref. [1]
HVP LO (e^+e^-)	Sec. 2.3.7	Eq. (2.33)	6931(40)	Refs. [2–7]
HVP NLO (e^+e^-)	Sec. 2.3.8	Eq. (2.34)	−98.3(7)	Ref. [7]
HVP NNLO (e^+e^-)	Sec. 2.3.8	Eq. (2.35)	12.4(1)	Ref. [8]
HVP LO (lattice, $udsc$)	Sec. 3.5.1	Eq. (3.49)	7116(184)	Refs. [9–17]
HLbL (phenomenology)	Sec. 4.9.4	Eq. (4.92)	92(19)	Refs. [18–30]
HLbL NLO (phenomenology)	Sec. 4.8	Eq. (4.91)	2(1)	Ref. [31]
HLbL (lattice, uds)	Sec. 5.7	Eq. (5.49)	79(35)	Ref. [32]
HLbL (phenomenology + lattice)	Sec. 8	Eq. (8.10)	90(17)	Refs. [18–30, 32]
QED	Sec. 6.5	Eq. (6.30)	116 584 718.931(104)	Refs. [33, 34]
Electroweak	Sec. 7.4	Eq. (7.16)	153.6(1.0)	Refs. [35, 36]
HVP (e^+e^- , LO + NLO + NNLO)	Sec. 8	Eq. (8.5)	6845(40)	Refs. [2–8]
HLbL (phenomenology + lattice + NLO)	Sec. 8	Eq. (8.11)	92(18)	Refs. [18–32]
Total SM Value	Sec. 8	Eq. (8.12)	116 591 810(43)	Refs. [2–8, 18–24, 31–36]
Difference: $\Delta a_\mu := a_\mu^{\text{exp}} - a_\mu^{\text{SM}}$	Sec. 8	Eq. (8.14)	279(76)	

Table 1: Summary of the contributions to a_μ^{SM} . After the experimental number from E821, the first block gives the main results for the hadronic contributions from Secs. 2 to 5 as well as the combined result for HLbL scattering from phenomenology and lattice QCD constructed in Sec. 8. The second block summarizes the quantities entering our recommended SM value, in particular, the total HVP contribution, evaluated from e^+e^- data, and the total HLbL number. The construction of the total HVP and HLbL contributions takes into account correlations among the terms at different orders, and the final rounding includes subleading digits at intermediate stages. The HVP evaluation is mainly based on the experimental Refs. [37–89]. In addition, the HLbL evaluation uses experimental input from Refs. [90–109]. The lattice QCD calculation of the HLbL contribution builds on crucial methodological advances from Refs. [110–116]. Finally, the QED value uses the fine-structure constant obtained from atom-interferometry measurements of the Cs atom [117].

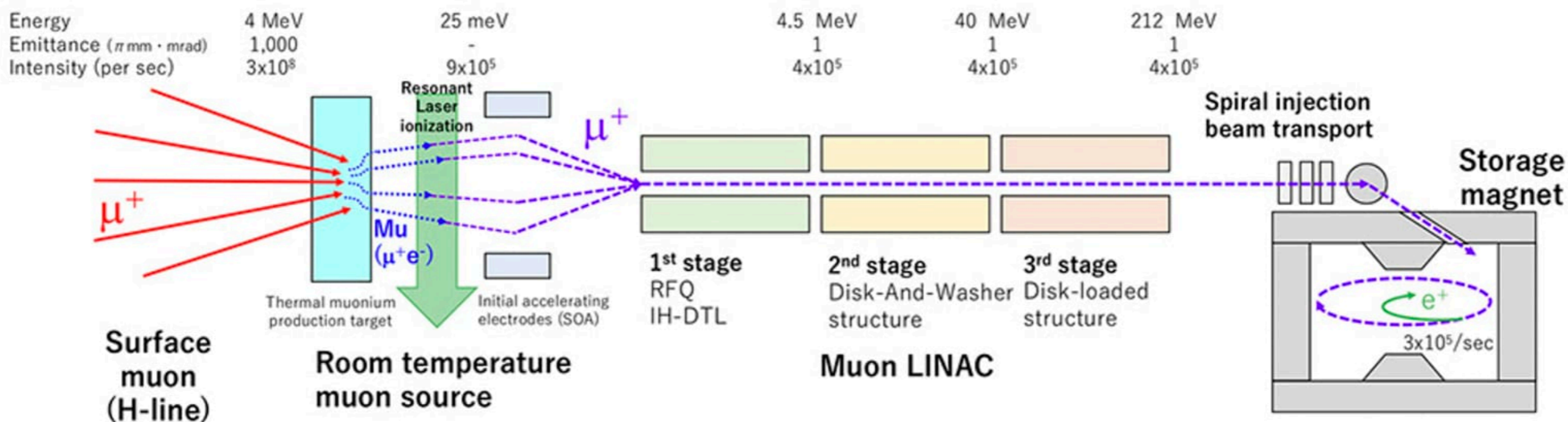




Muon anomalous magnetic moment $a_\mu \times 10^9 - 1165900$

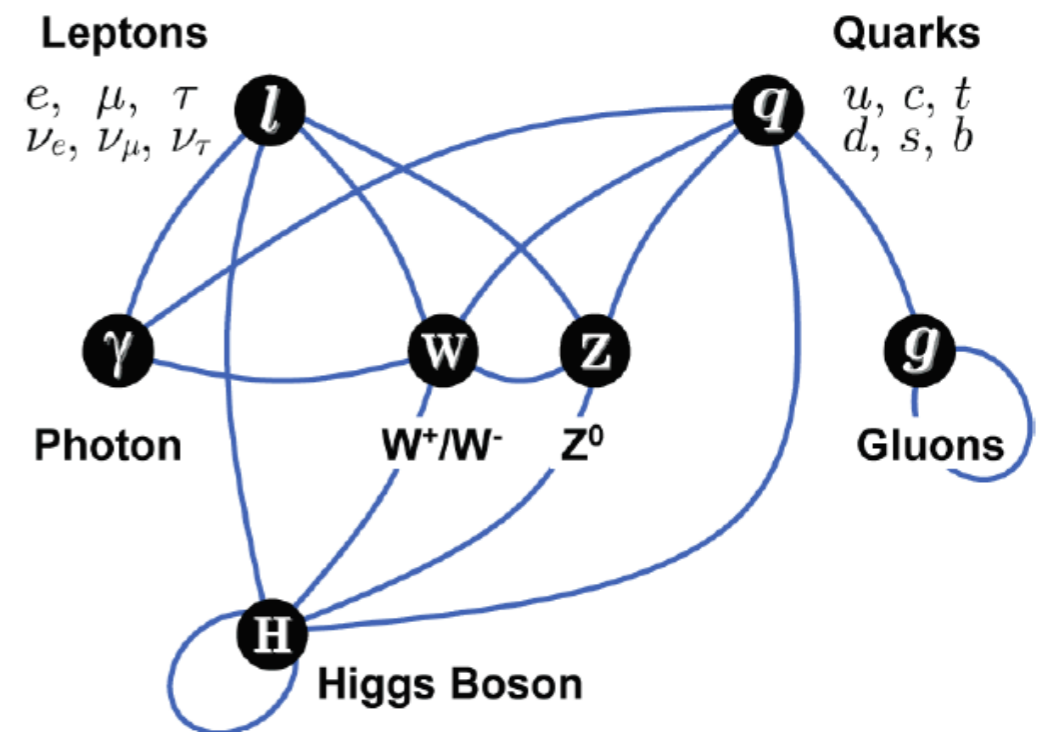
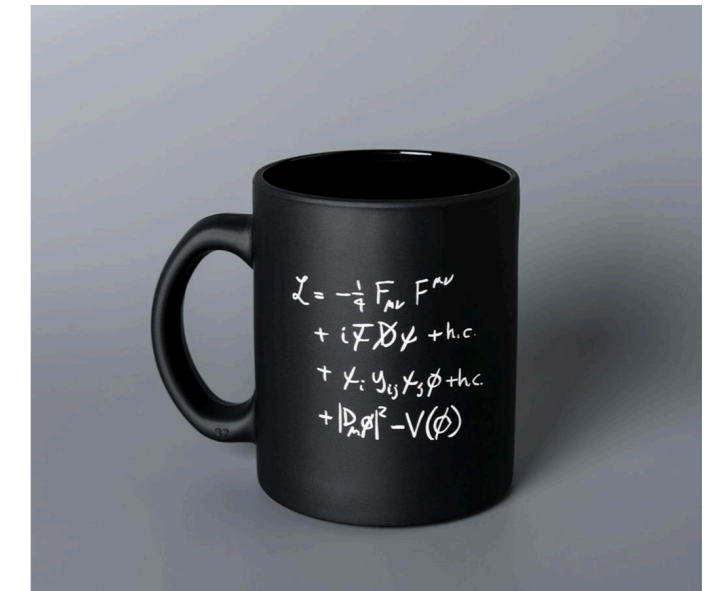


J-PARC muon ***g-2/EDM*** experiment

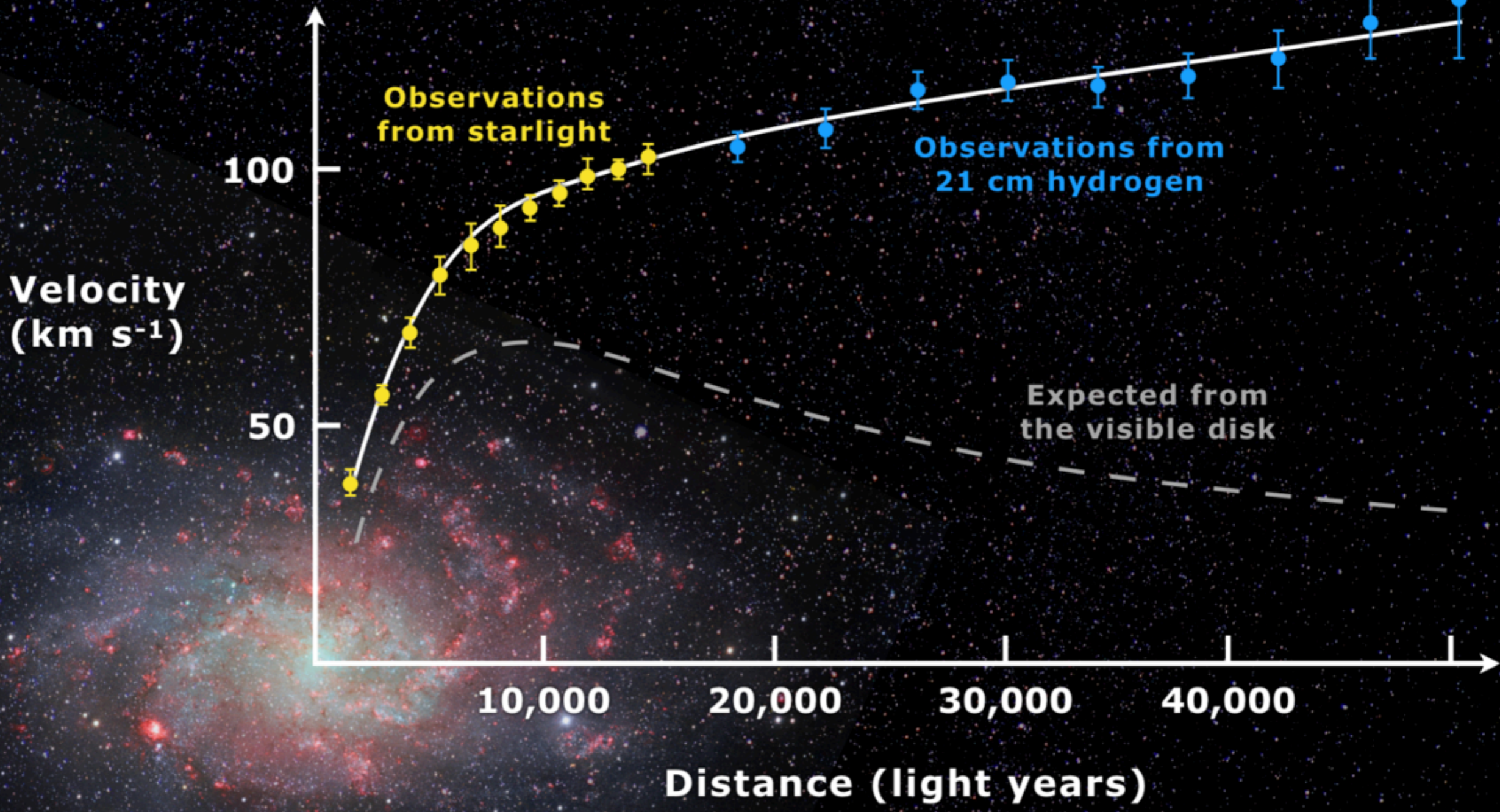


КАРТИНА ЭЛЕМЕНТАРНЫХ ЧАСТИЦ:

	Fermions			Bosons	
Quarks	u up	c charm	t top	γ photon	Force carriers
	d down	s strange	b bottom	Z Z boson	
Leptons	ν_e electron neutrino	ν_μ muon neutrino	ν_τ tau neutrino	W W boson	
	e electron	μ muon	τ tau	g gluon	
				Higgs boson	



Source: AAAS



Velocity
(km s^{-1})

100

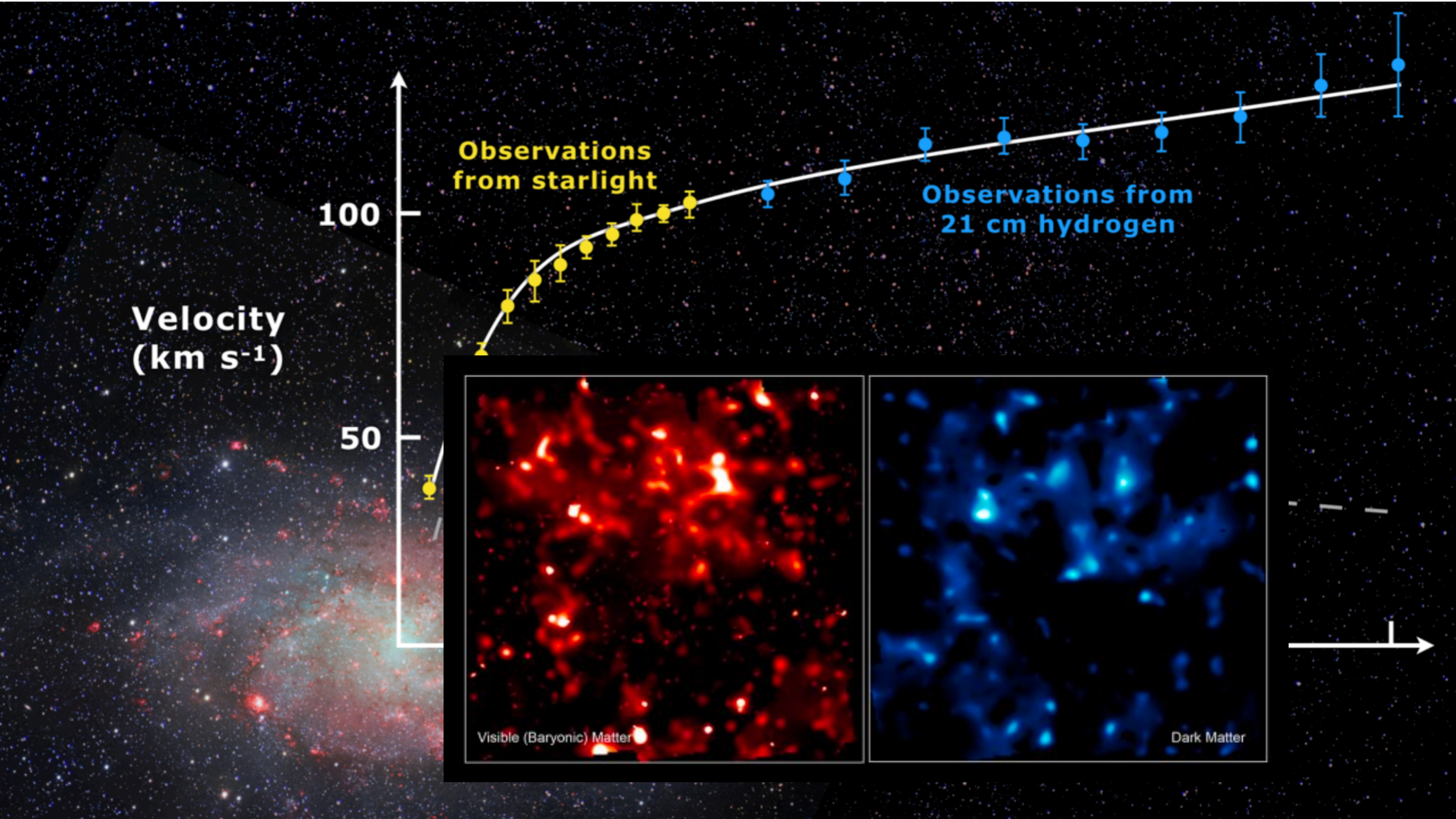
50

Observations
from starlight

Observations from
21 cm hydrogen

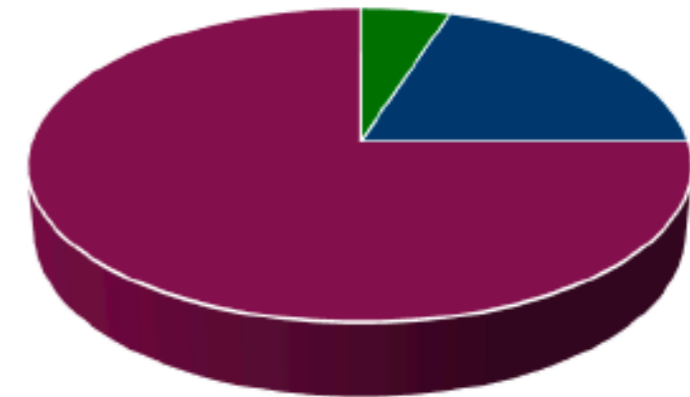
Visible (Baryonic) Matter

Dark Matter



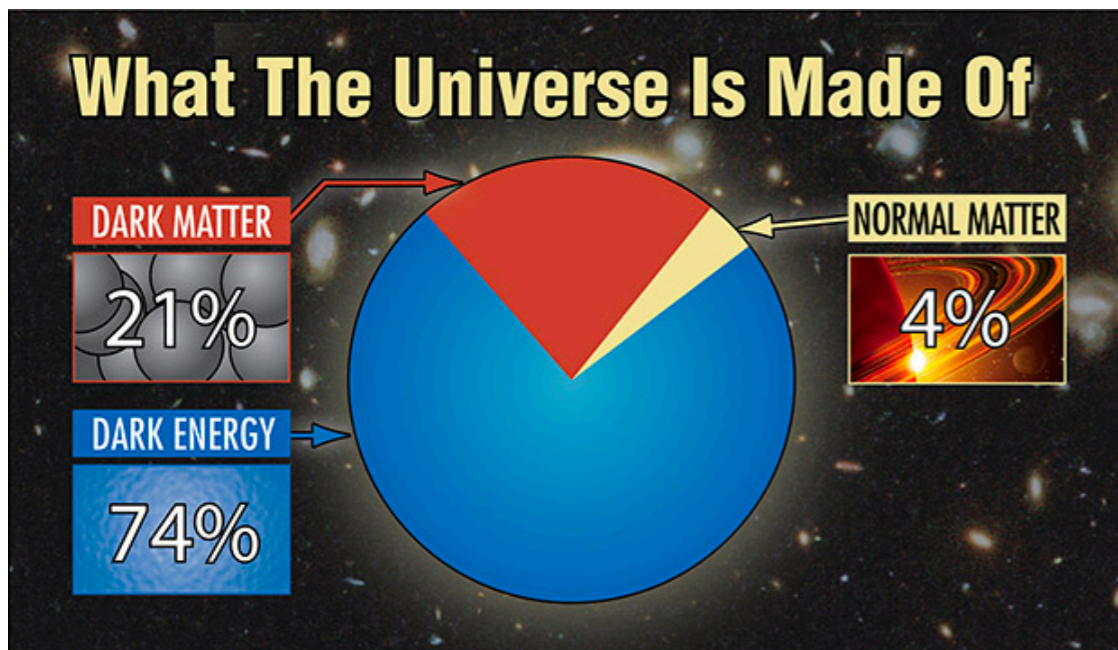
Physics Beyond the Standard Model

- Dark Matter existence established at cosmological scales
 - New weakly interacting particles
- Neutrinos not exactly massless
 - Right-handed (sterile) neutrinos
- Matter anti-matter asymmetry
 - Additional CP violating interactions



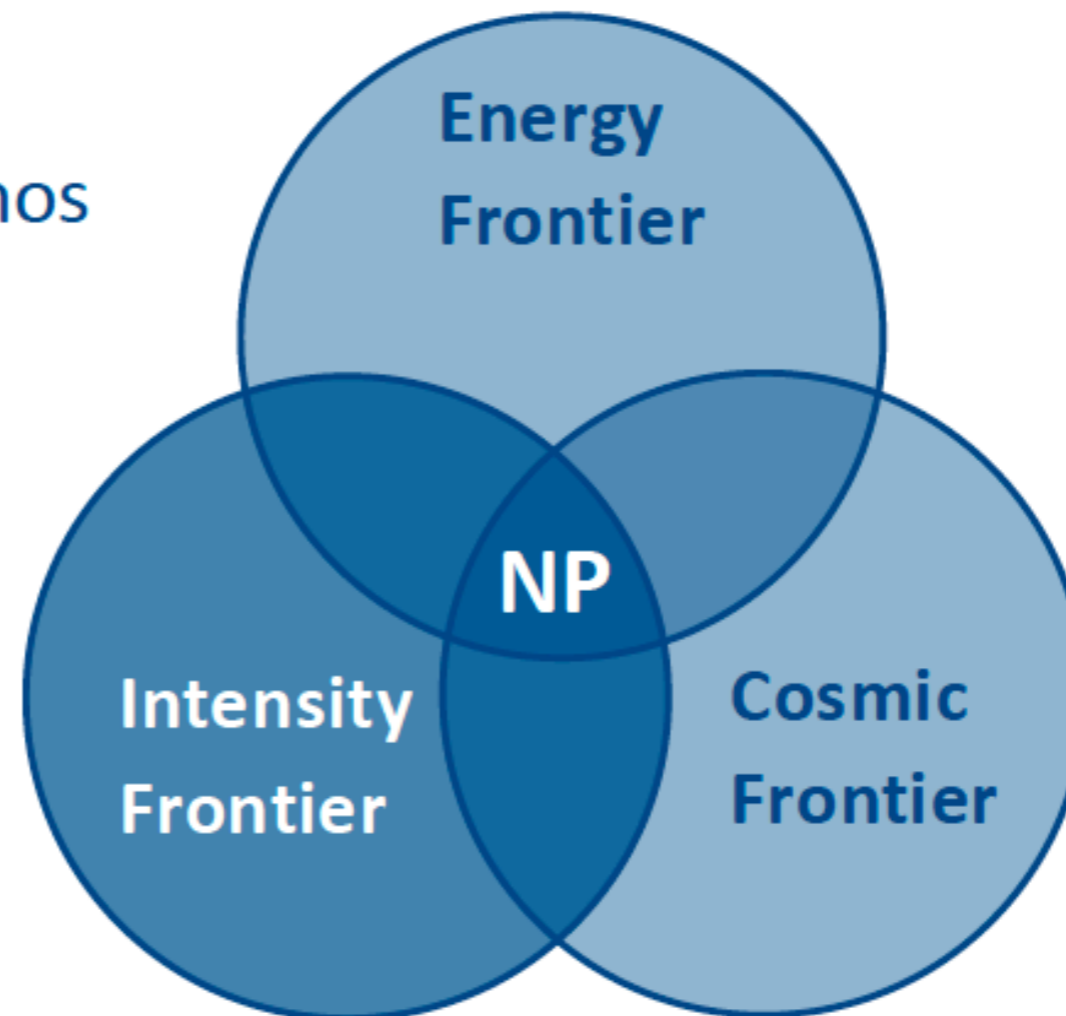
- SM
- Dark Matter
- Dark Energy

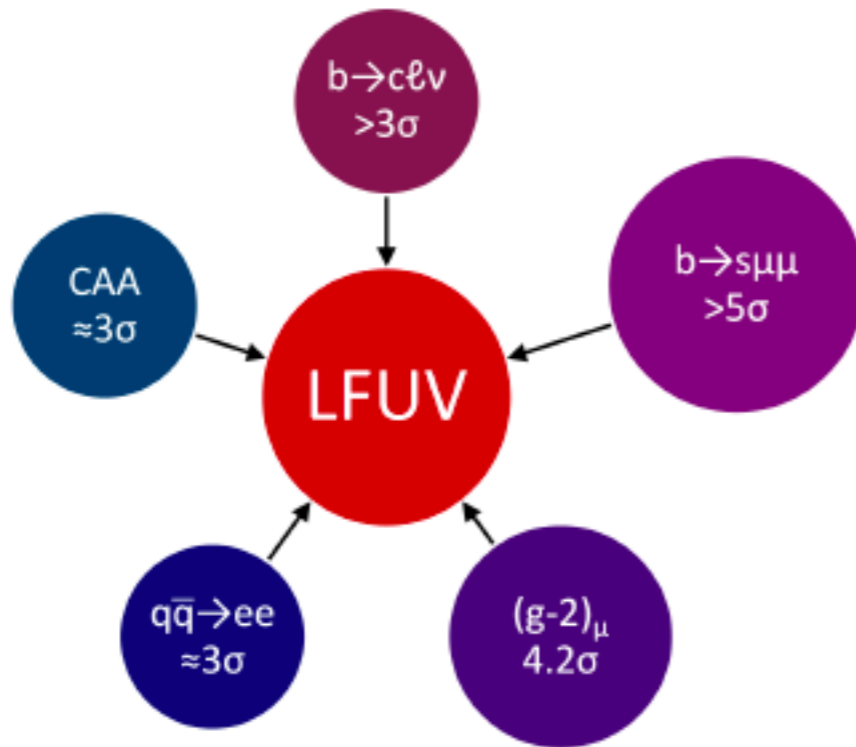
The SM must be extended!
What is the underlying fundamental theory?



Discovering New Physics

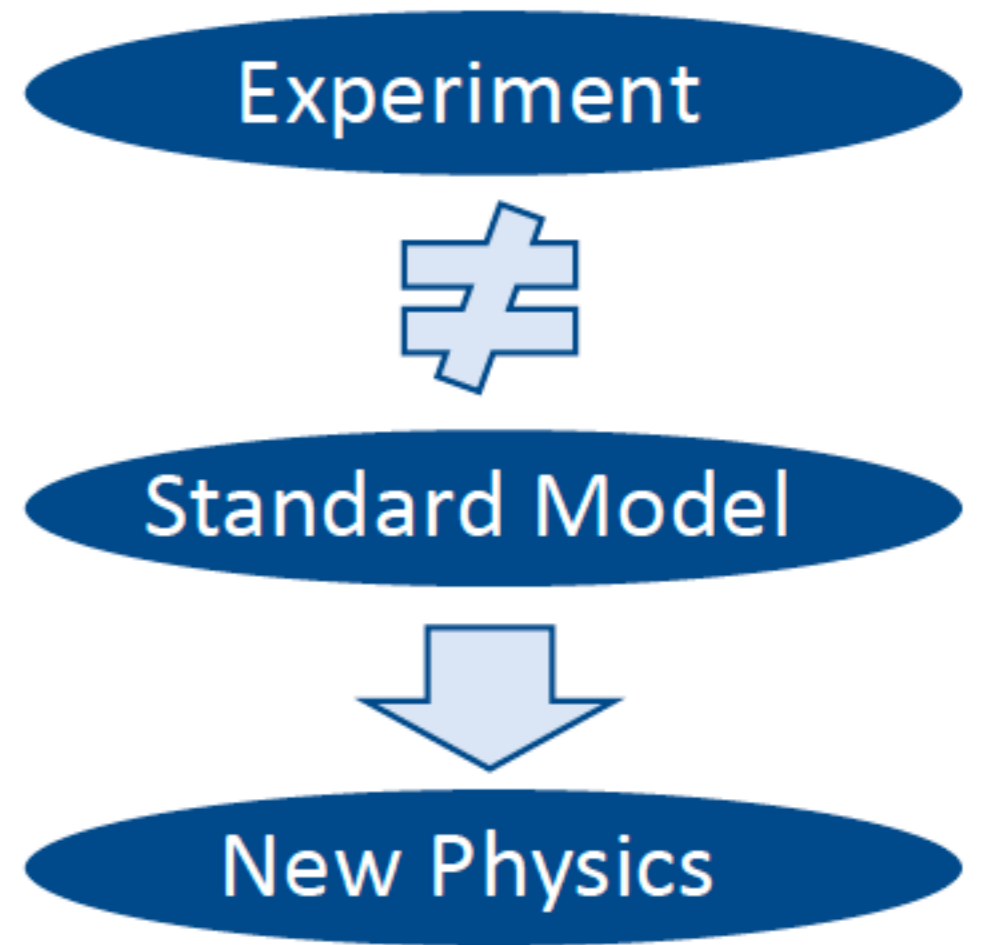
- **Cosmic Frontier**
 - Cosmic rays and neutrinos
 - Dark Matter
 - Dark Energy
- **Energy Frontier**
 - LHC
 - Future colliders
- **Intensity Frontier**
 - Flavour
 - Neutrino-less double- β decay
 - Test of fundamental symmetries
 - Proton decay





Different hints for the violation of LFU, with size of the spheres reflecting the significance of the respective tension.

A. Crivellin and M. Hoferichter.
 Science 374(2021) no.6571, 1051



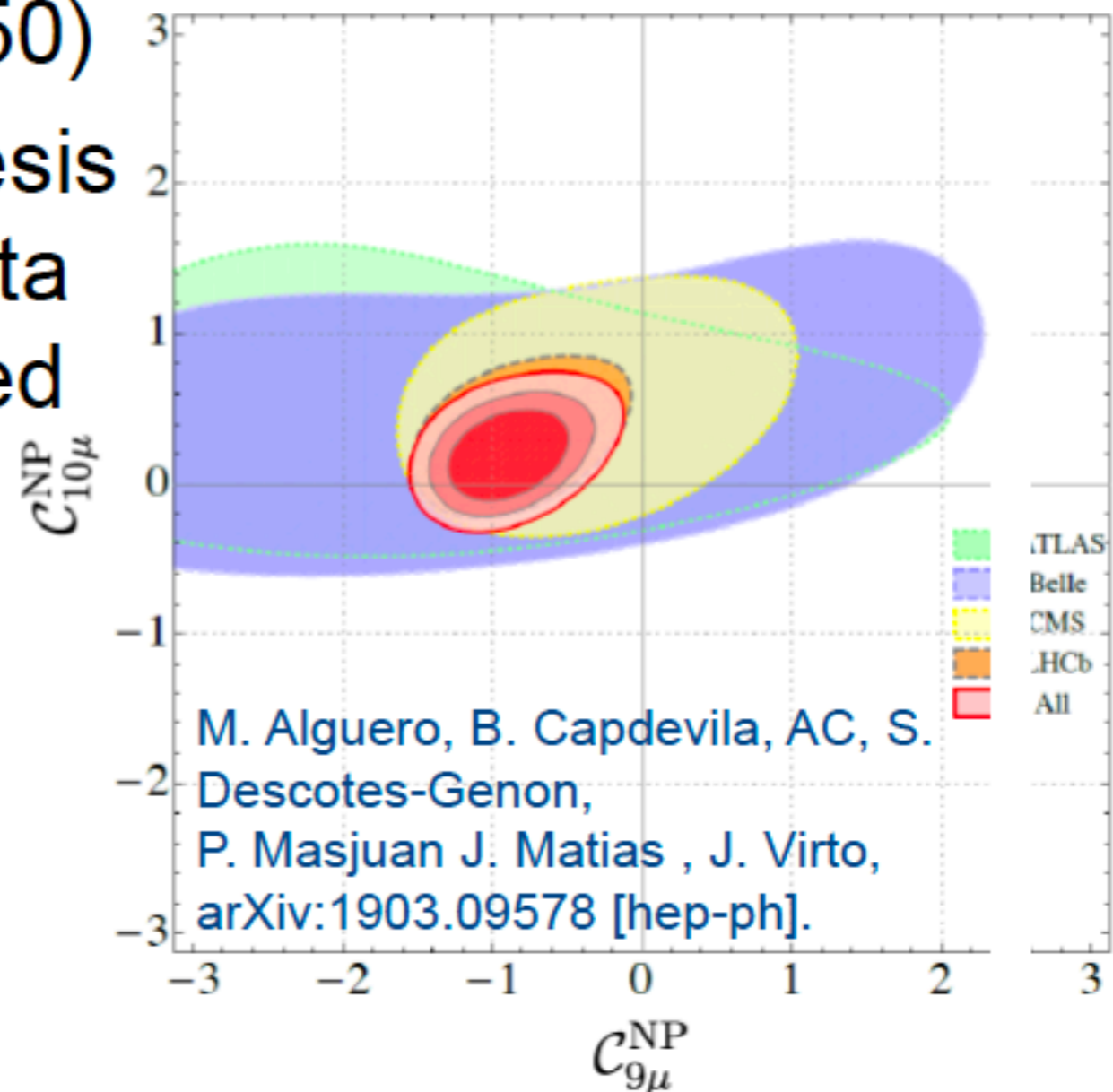
LFV Channel	Current limit	Projection
$\mu \rightarrow e\gamma$	4.2×10^{-13} [MEG Coll. (2016)]	6×10^{-14} [MEGII Coll. (2018)]
$\mu \rightarrow 3e$	1.0×10^{-12} [SINDRUM Coll. (1988)]	1×10^{-16} [Perrevoort, Mu3e (2018)]
$\mu \rightarrow ea, m_a < 13 \text{ MeV}$	5.8×10^{-5} [Bayes <i>et al</i> (2014)]	1×10^{-8} [Perrevoort, Mu3e (2018)]
$\mu \rightarrow ea, m_a > 13 \text{ MeV}$	9.0×10^{-6}	
$\mu \rightarrow ea\gamma$	1.1×10^{-9} [Bolton <i>et al</i> (1988)]	
$\mu \rightarrow e\gamma\gamma$	7.2×10^{-11} [LAMPF Coll (1986)]	
$\mu N \rightarrow eN$	7.0×10^{-13} [SINDRUM-II (2006)]	1×10^{-17} [Mu2e (2014)] [COMET (2020)]

Global Fit to $b \rightarrow s \mu^+ \mu^-$ Data

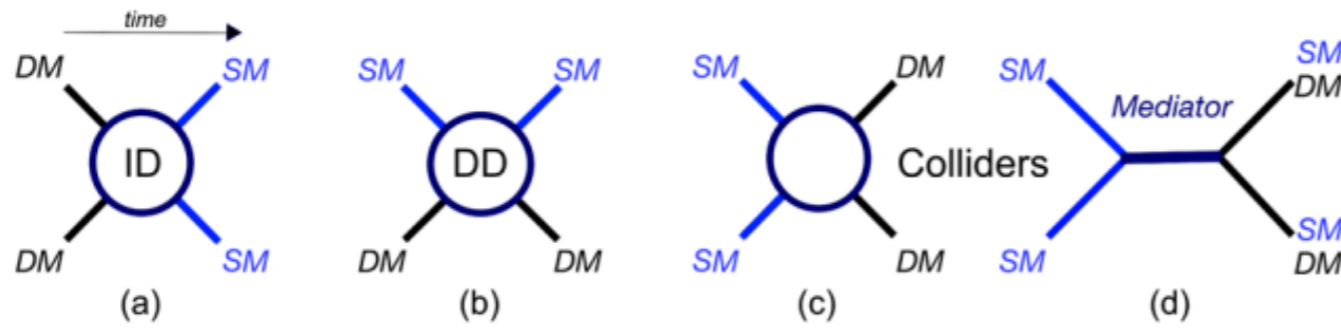
- Perform global model independent fit to include all observables (≈ 150)
- Several NP hypothesis give a good fit to data significantly preferred over the SM hypothesis

$$O_9 = \bar{s} \gamma^\mu P_L b \bar{\ell} \gamma_\mu \ell$$

$$O_{10} = \bar{s} \gamma^\mu P_L b \bar{\ell} \gamma_\mu \gamma^5 \ell$$

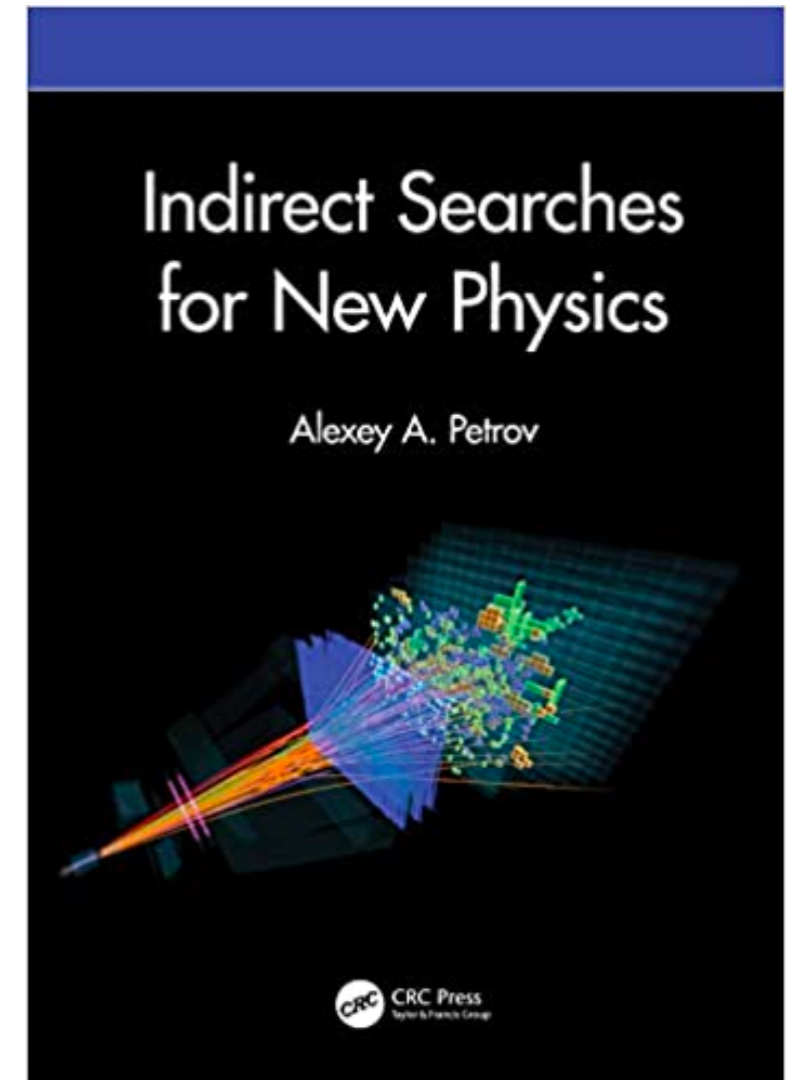


Fit is 5-6 σ better than the SM



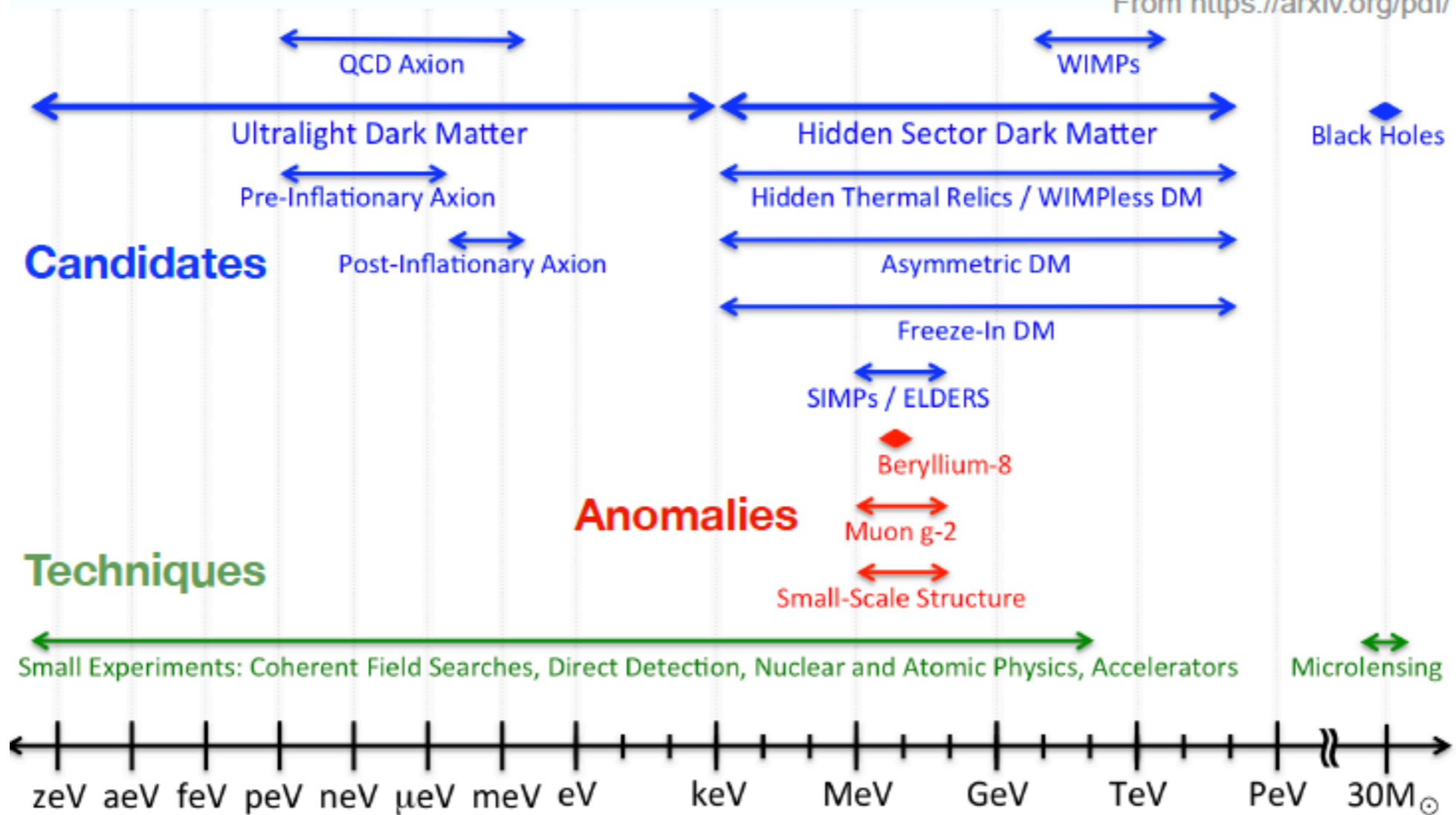
There have been four popular portals:

- (1) Vector portal
- (2) Axion portal:
- (3) Higgs portal:
- (4) Neutrino portal



Dark sectors landscape

From <https://arxiv.org/pdf/1707.04591.pdf>



Broad mass range \Rightarrow can not be covered by a single experiment

Complementary searches involving different techniques

Search of DM

Precision experiments:

- 1) $g-2$ of leptons
- 2) EDM of leptons, neutrons and etc
- 3) Atomic clock
- 4) Resonator experiments

Search at LHC and other collider experiments :

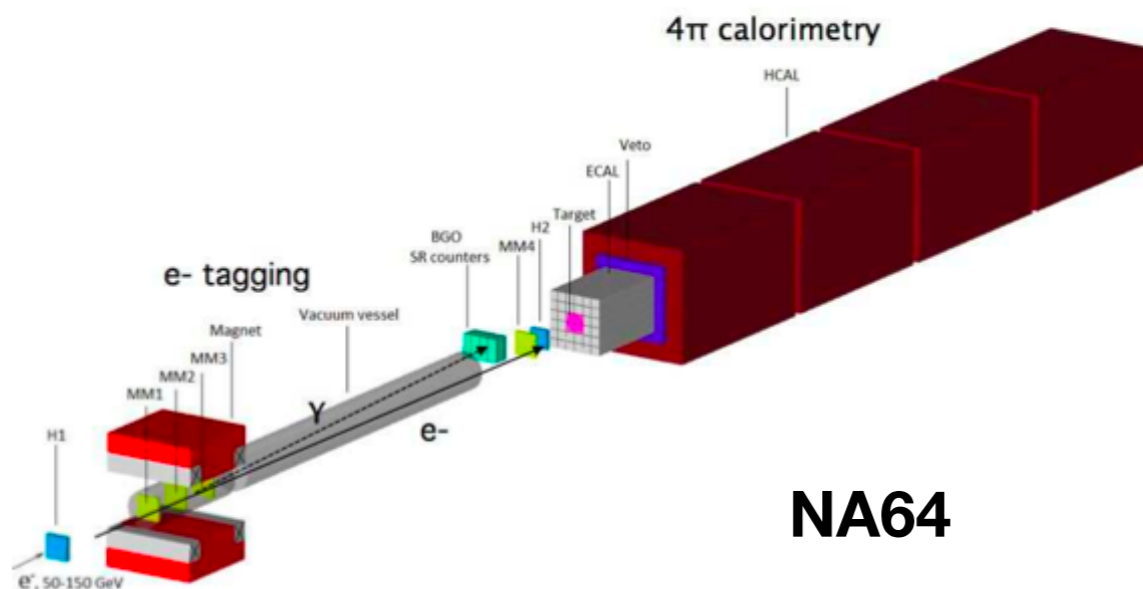
- 1) CMS, Atlas
- 2) LHCb
- 3) NA62
- 4) GlueX

Missing Energy and Missing momenta experiments

- 1) NA64 at SPS CERN
- 2) LDMX

In superconductors

LFV process



Search of DM



$$\mathcal{L} \supset -\frac{1}{4}F'^{\mu\nu}F'_{\mu\nu} + \frac{m_{A'}^2}{2}A'_\mu A'^\mu - A'_\mu(\epsilon e J_{EM}^\mu + g_D J_D^\mu),$$

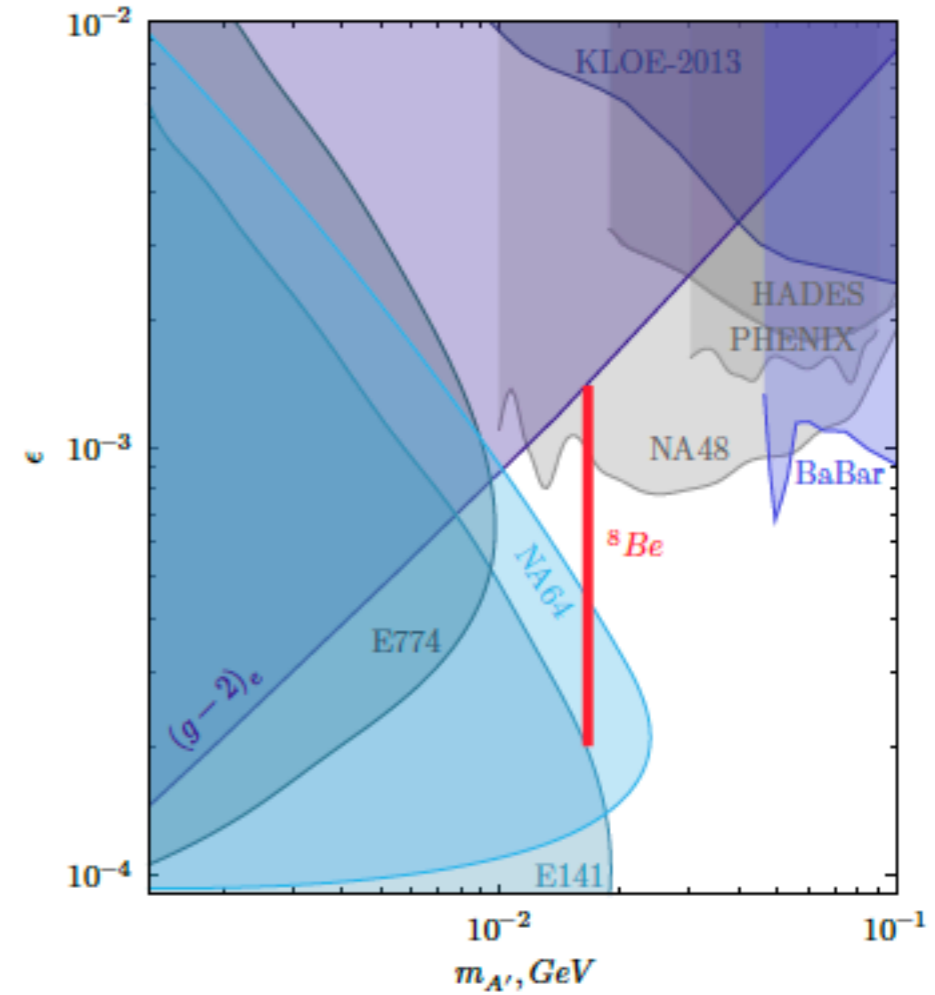
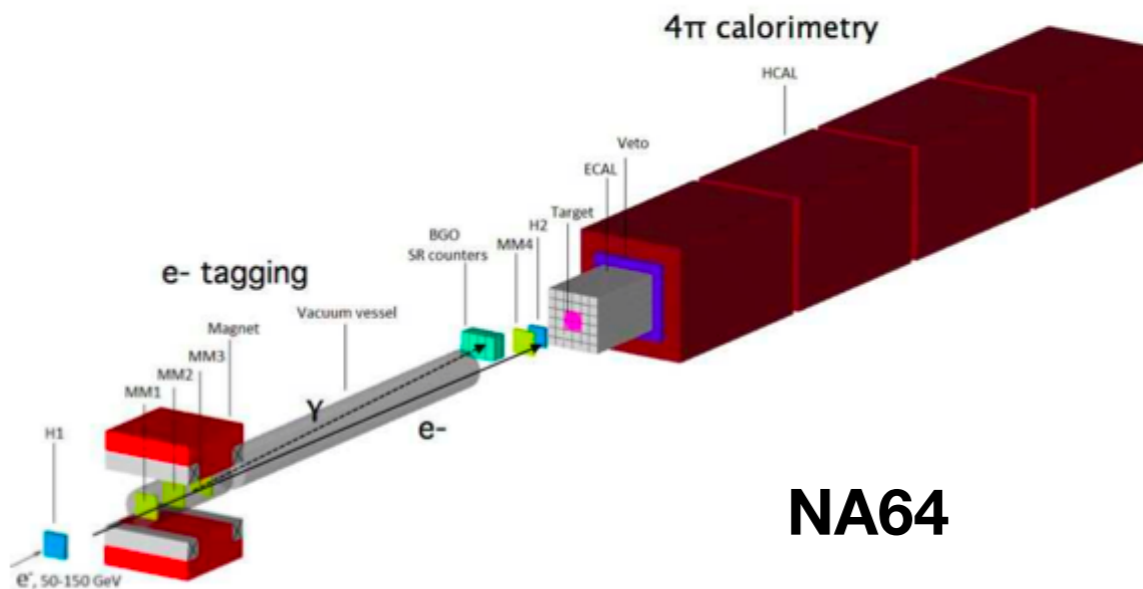


FIG. 3. The 90% C.L. exclusion areas in the $(m_X; \epsilon)$ plane from the NA64 experiment (blue area). For the mass of 16.7 MeV, the $X - e^-$ coupling region excluded by NA64 is $1.3 \times 10^{-4} < \epsilon_e < 4.2 \times 10^{-4}$. The allowed range of ϵ_e explaining the ${}^8\text{Be}^*$ anomaly (red area) [2, 3], constraints on the mixing ϵ from the experiments E141 [22], E774 [25], BaBar [40], KLOE [45], HADES [48], PHENIX [49], NA48 [51], and bounds from the electron anomalous magnetic moment $(g-2)_e$ [71] are also shown.



NA64

LDMX

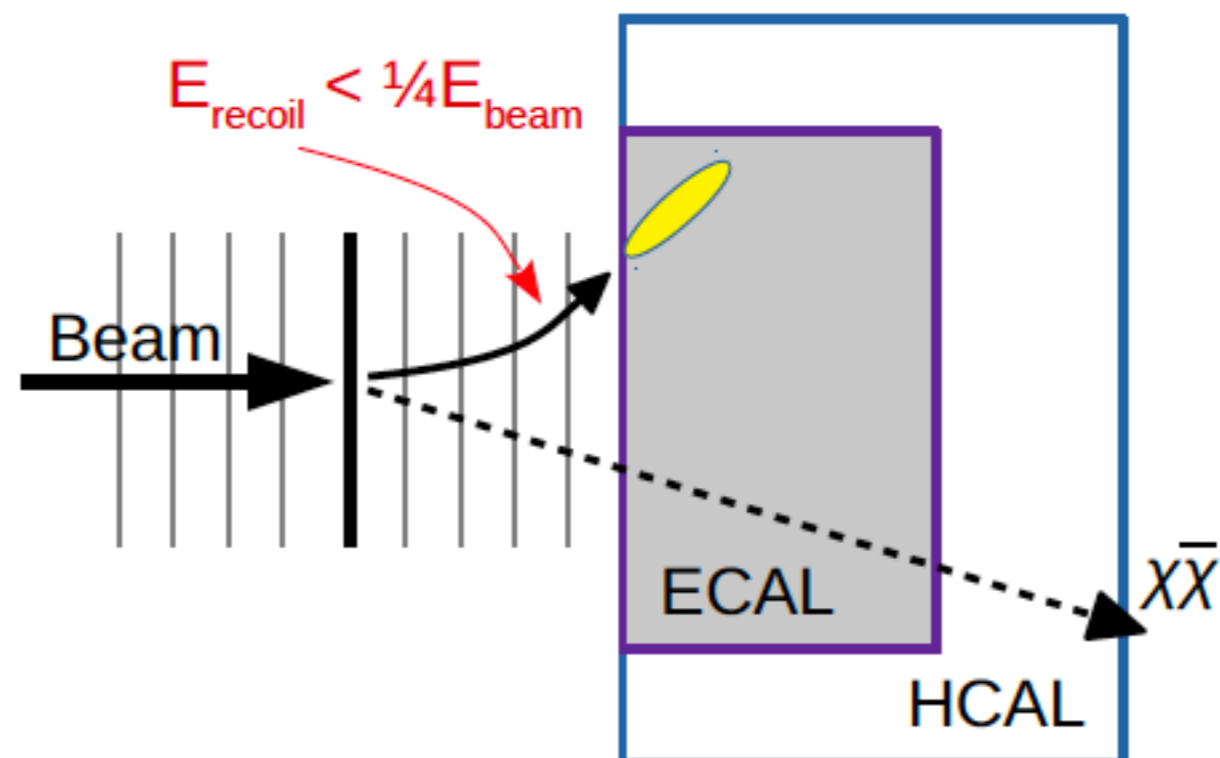
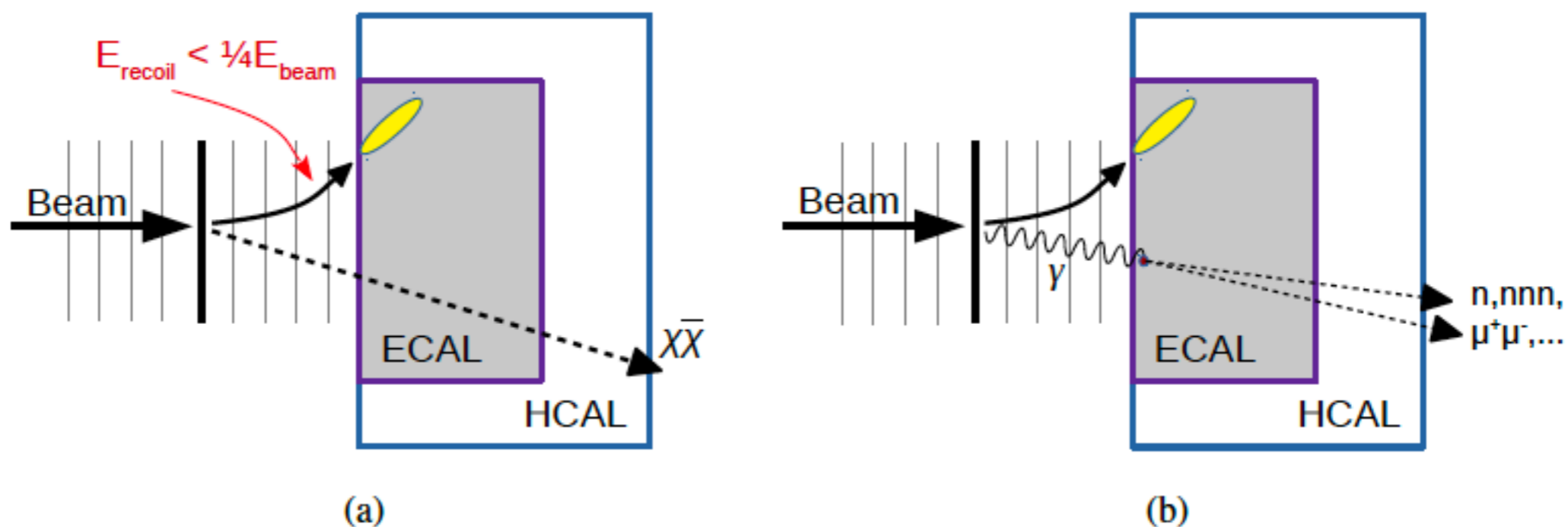
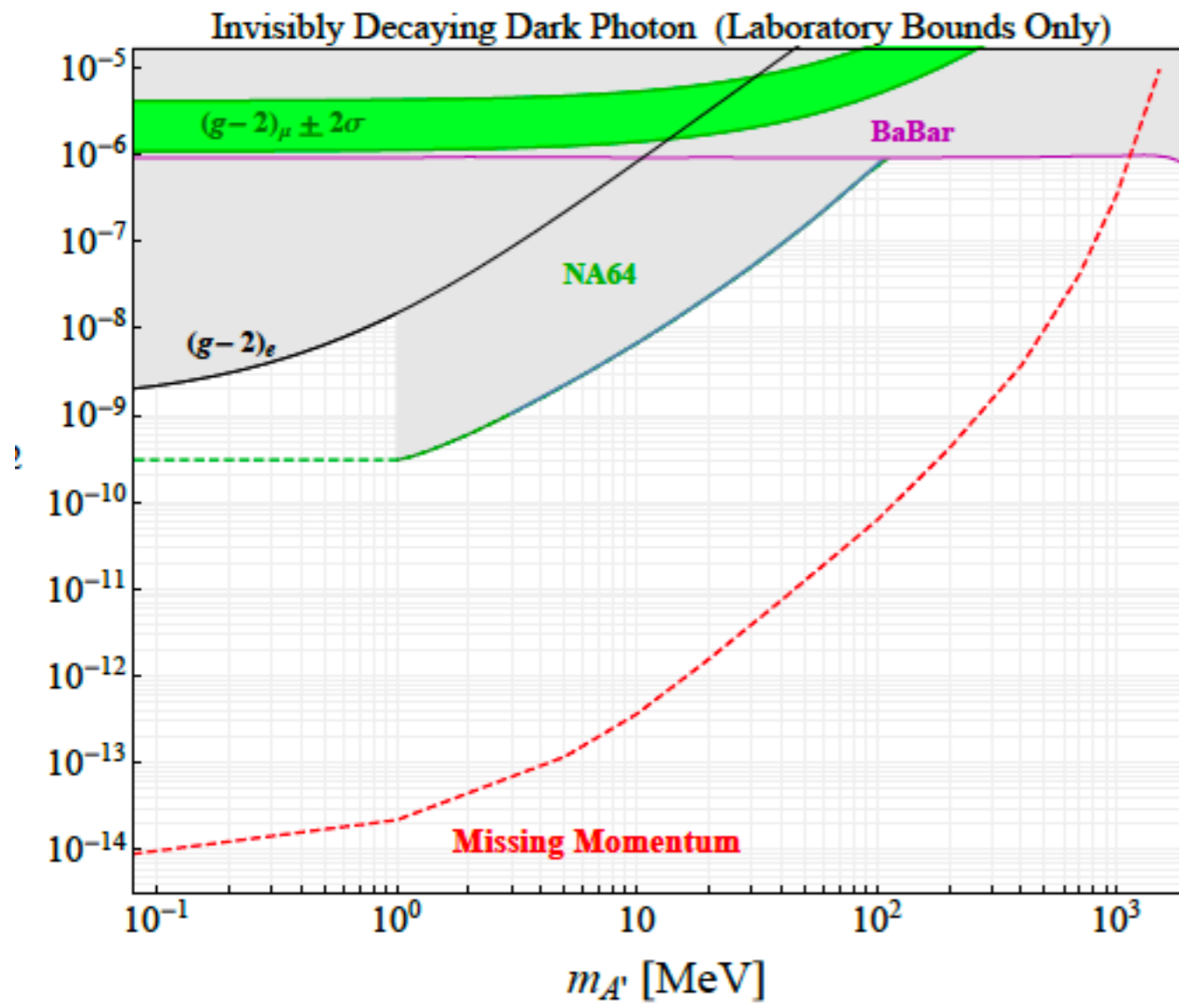


FIG. 8: Conceptual drawing of the LDMX experiment, showing the electron beam passing through a tagging tracker, impacting on a thin tungsten target, the recoil tracker, the electromagnetic calorimeter, and hadron calorimeter.



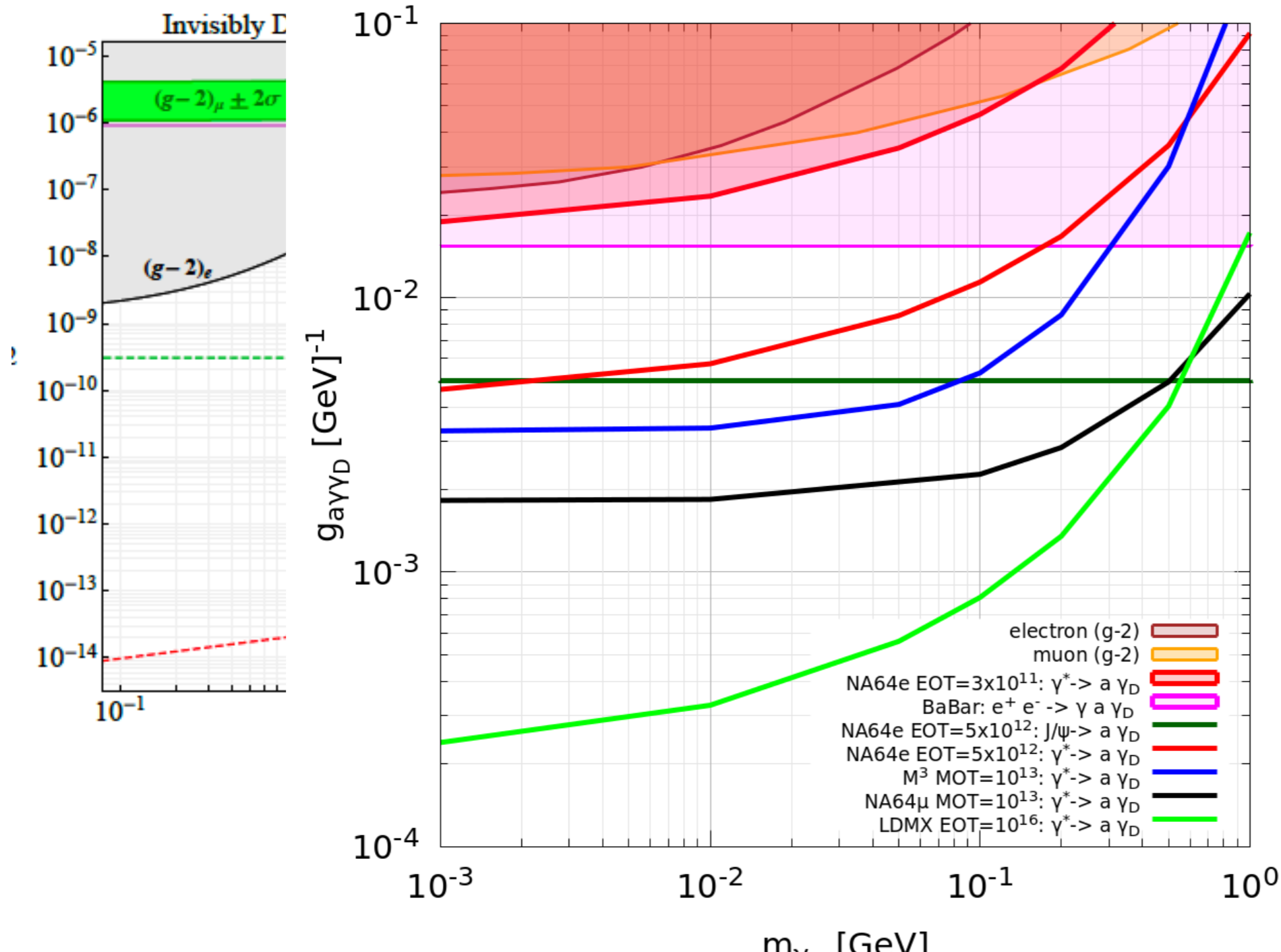
The general Lagrangian for this family of models contains

$$\mathcal{L} \supset -\frac{1}{4}F'^{\mu\nu}F'_{\mu\nu} + \frac{m_{A'}^2}{2}A'_\mu A'^\mu - A'_\mu(\epsilon e J_{EM}^\mu + g_D J_D^\mu),$$

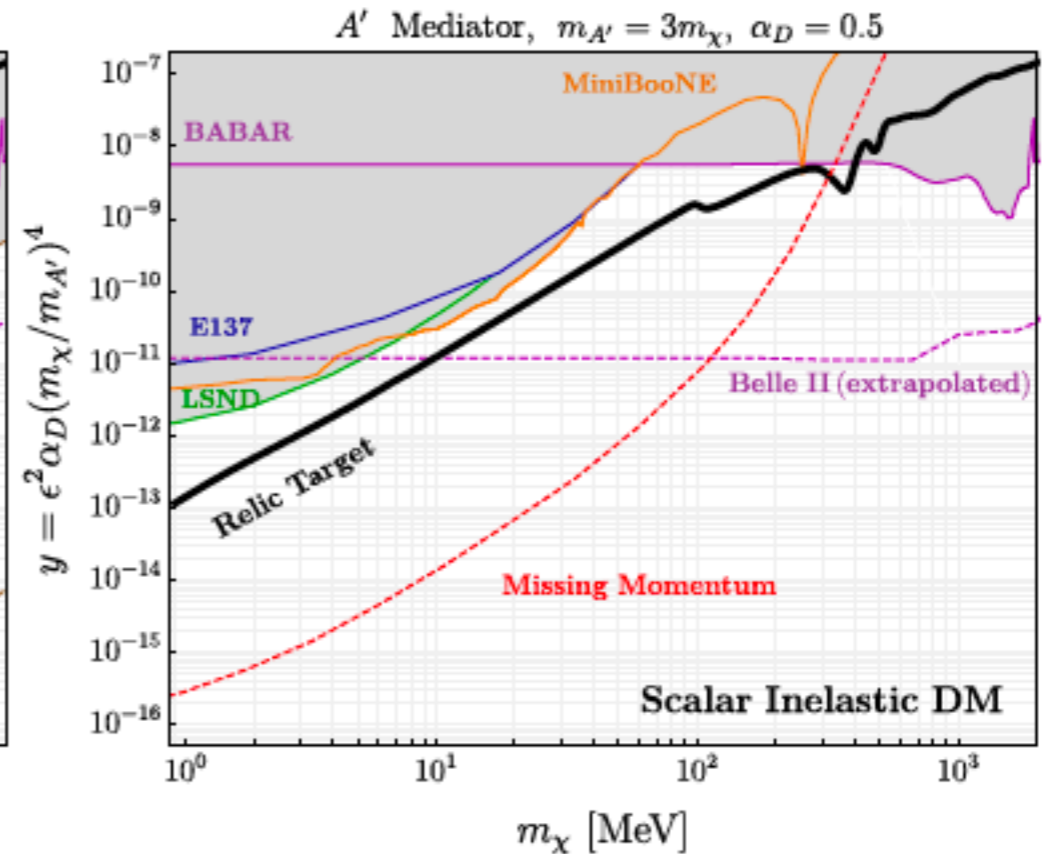
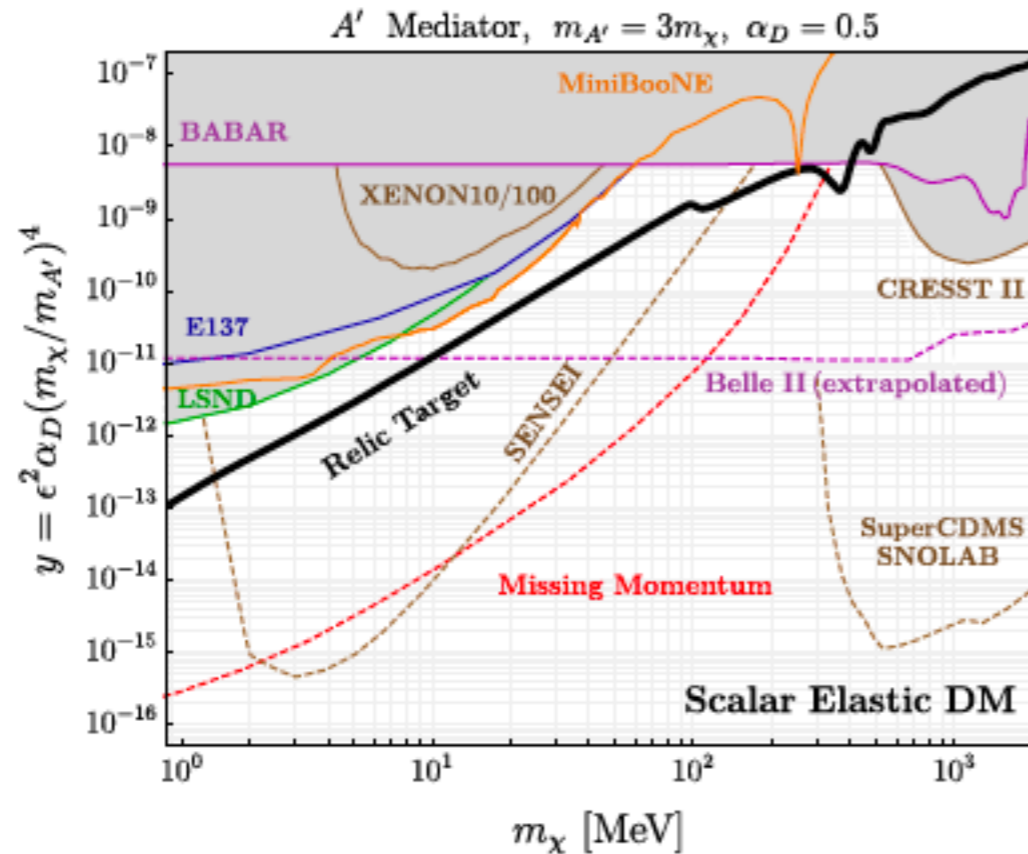
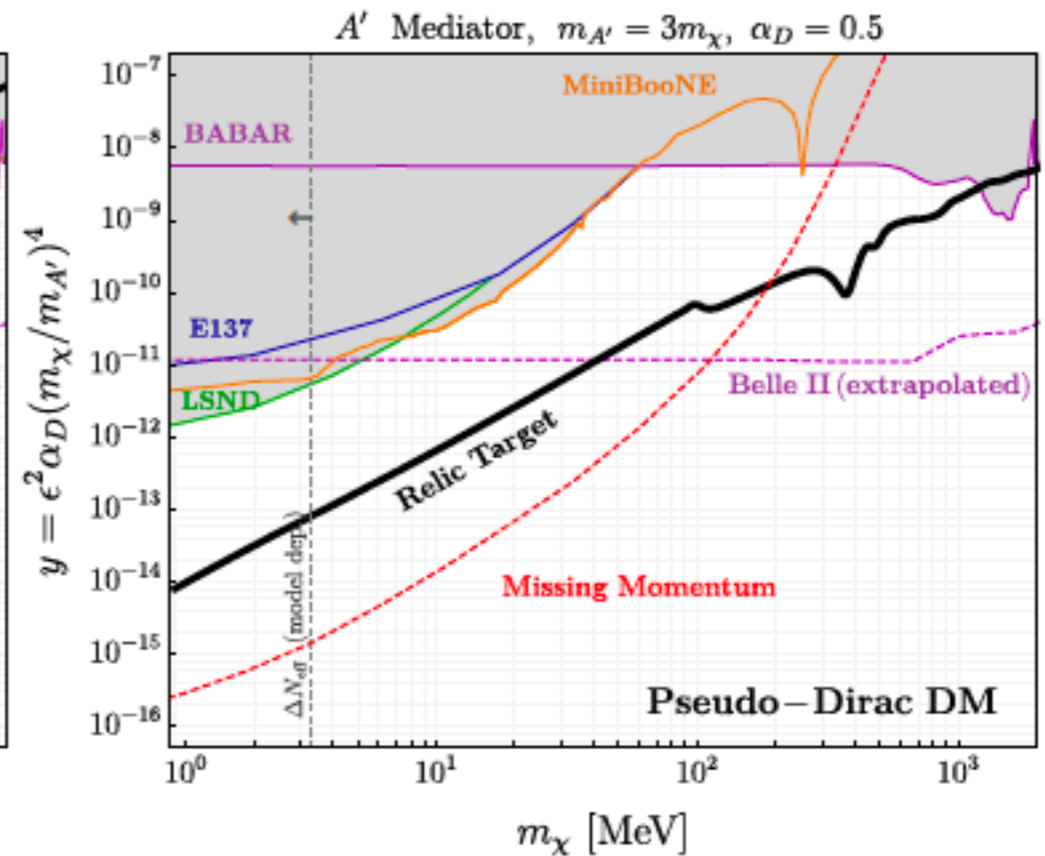
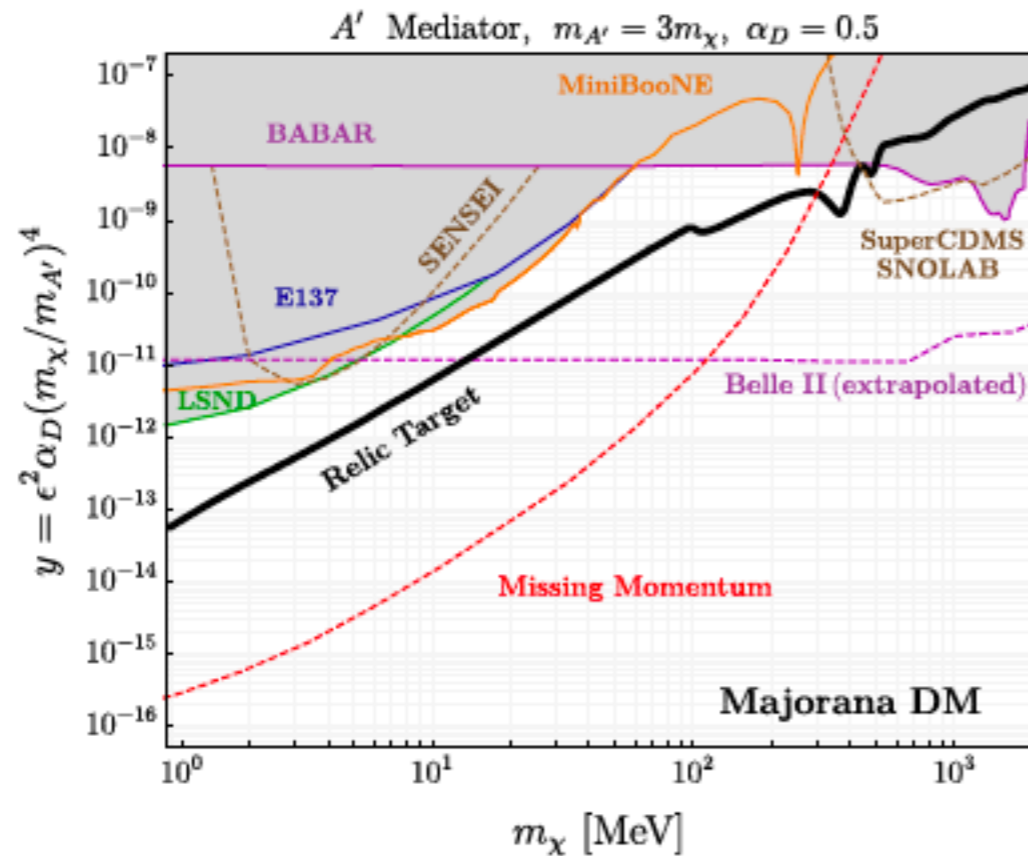


The general Lagrangian for this family of models contains

$$\mathcal{L}_{\text{dark axion portal}} = \frac{g_{a\gamma_D\gamma_D}}{4} a F'_{\mu\nu} \widetilde{F}'^{\mu\nu} + \frac{g_{a\gamma\gamma_D}}{2} a F_{\mu\nu} \widetilde{F}'^{\mu\nu}$$



LDMX



Neutron EDM – Situation & Perspective

► **First Ramsey measurement**

Smith, Purcell & Ramsey, Phys. Rev. 108, 120 (1957)

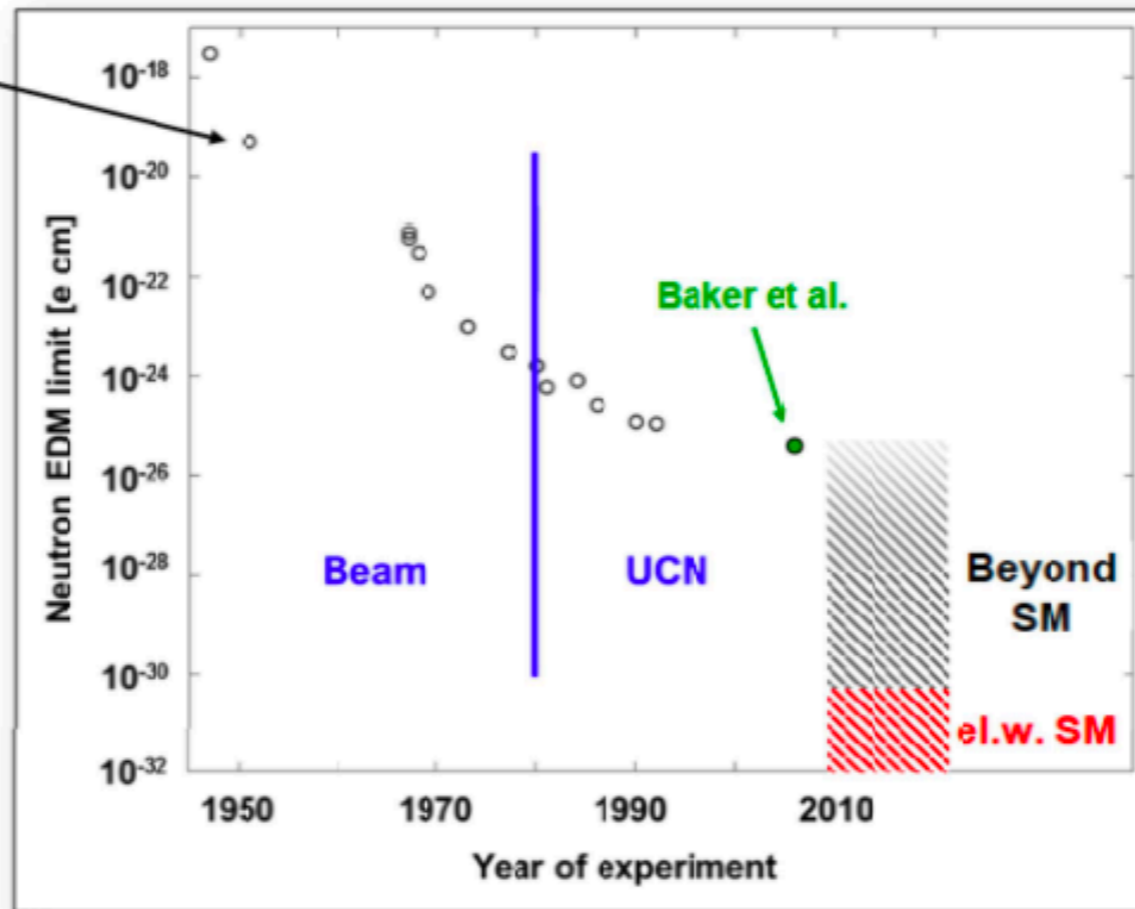
► **Current limit:**

$$|d_n| < 2.9 \times 10^{-26} \text{ e cm} \quad (90\% \text{ CL})$$

Baker et al., PRL 97, 131801 (2006)

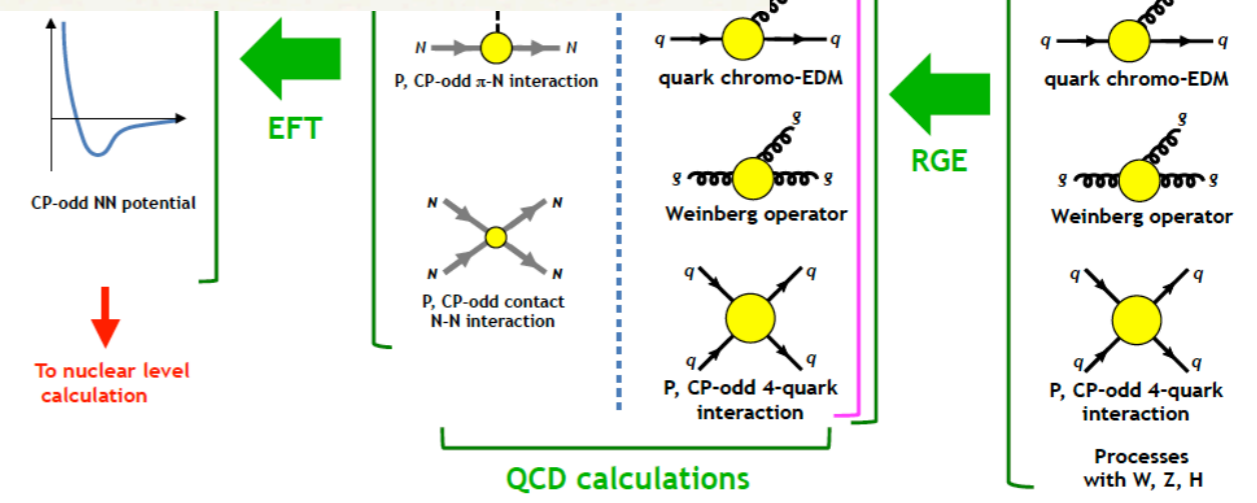
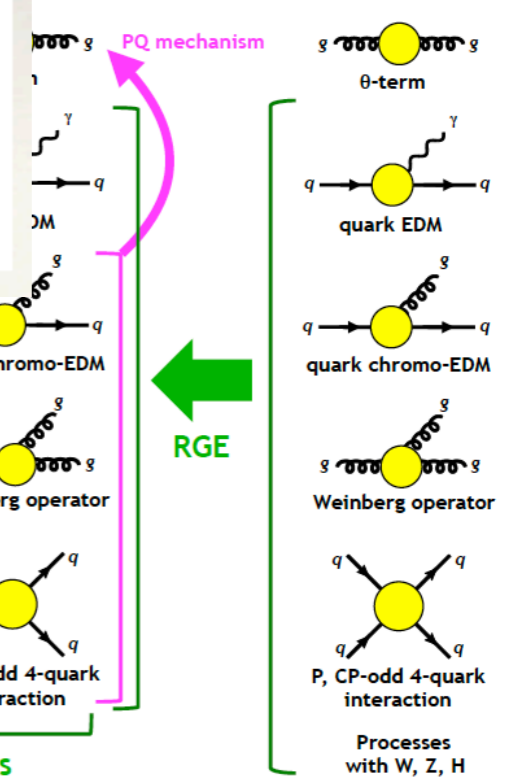
► **Sensitivity:**

$$\sigma(d_n) \propto \frac{1}{E T \sqrt{N}}$$



rel

CPV QCD TeV scale CPV QCD



Neutron EDM – Situation & Perspective

► **First Ramsey measurement**

Smith, Purcell & Ramsey, Phys. Rev. 108, 120 (1957)

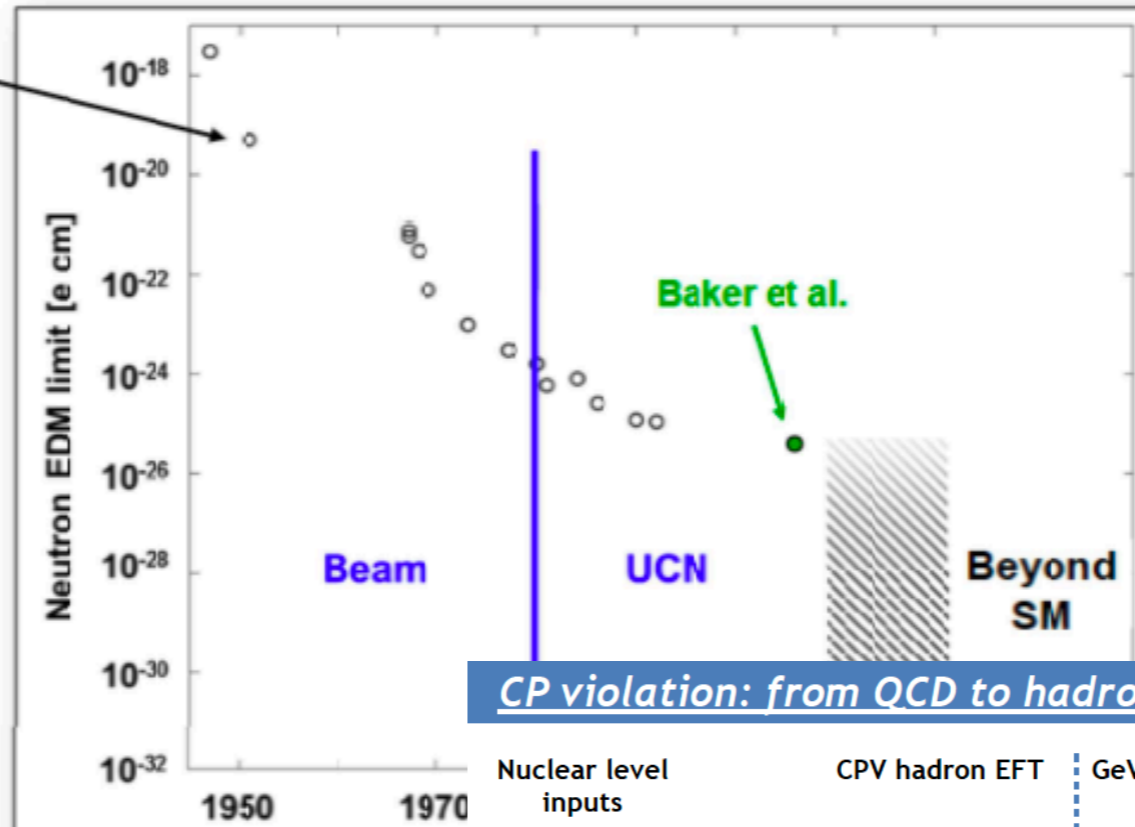
► **Current limit:**

$$|d_n| < 2.9 \times 10^{-26} \text{ e cm} \quad (90\% \text{ CL})$$

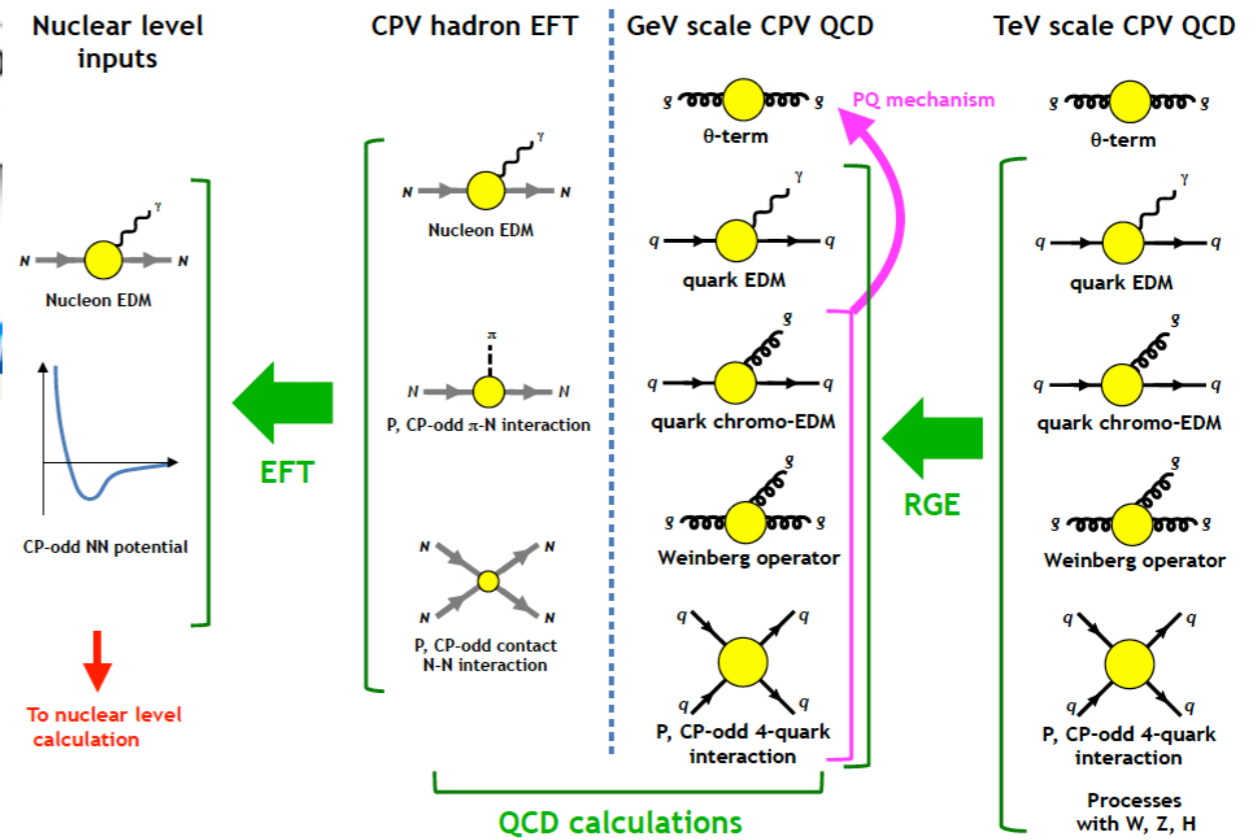
Baker et al., PRL 97, 131801 (2006)

► **Sensitivity:**

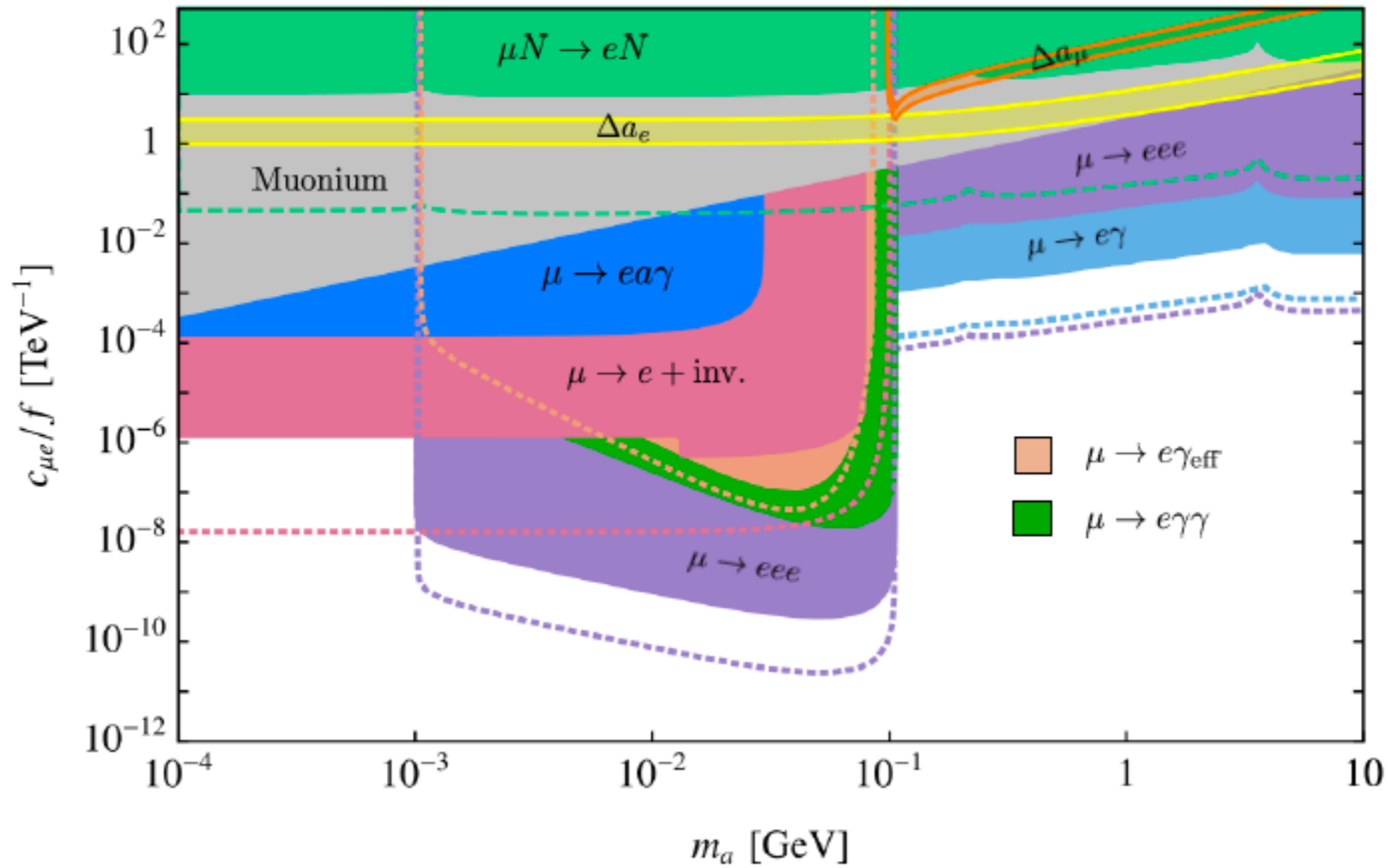
$$\sigma(d_n) \propto \frac{1}{E T \sqrt{N}}$$

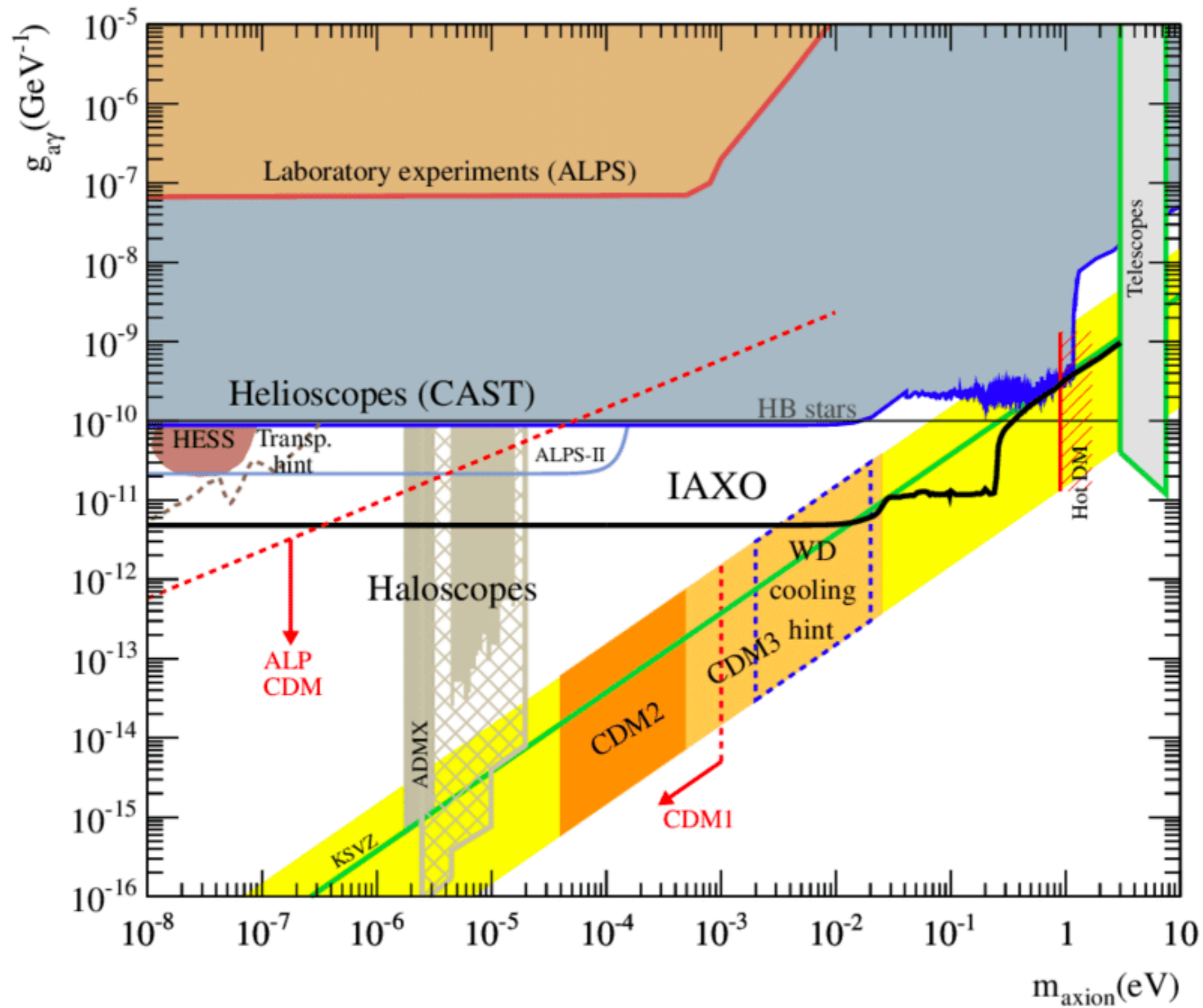


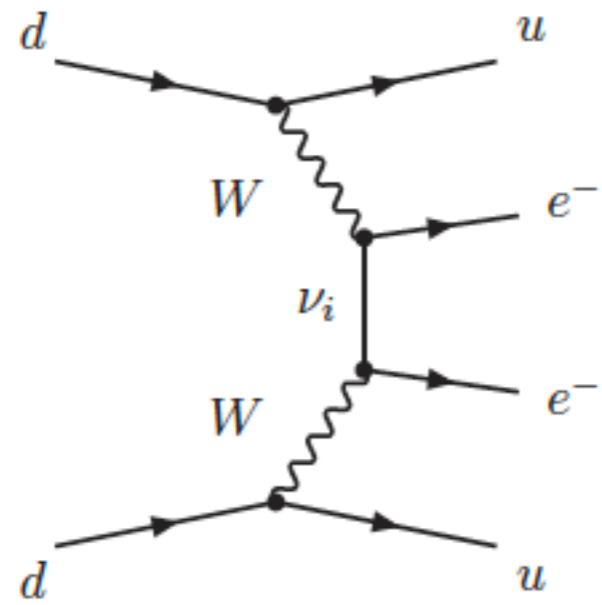
CP violation: from QCD to hadron level



$$\mathcal{L}_{eff}^{D \leq 5} = \frac{1}{2}(\partial_\mu a)(\partial^\mu a) - \frac{m_{a,0}^2}{2}a^2 + \frac{\partial_\mu a}{\Lambda} \gamma_\mu \bar{\ell} (K_E P_L + K_e P_R) \ell + e^2 c_{\gamma\gamma}^{\text{eff}} \frac{a}{\Lambda} F_{\mu\nu} \tilde{F}^{\mu\nu}$$







Quark-level transition that induces neutrinoless double beta decay.

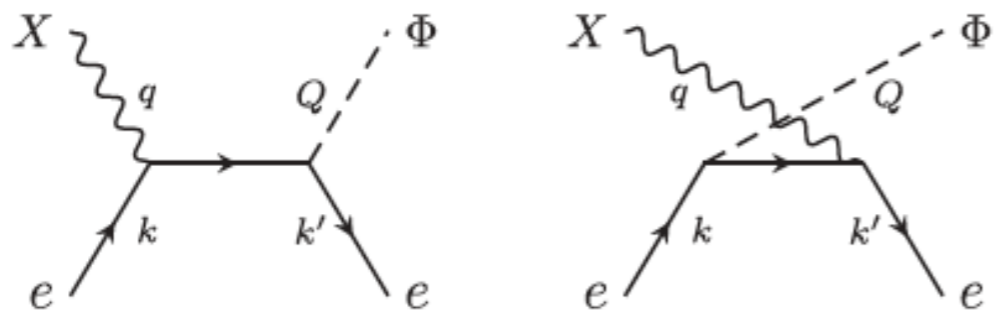
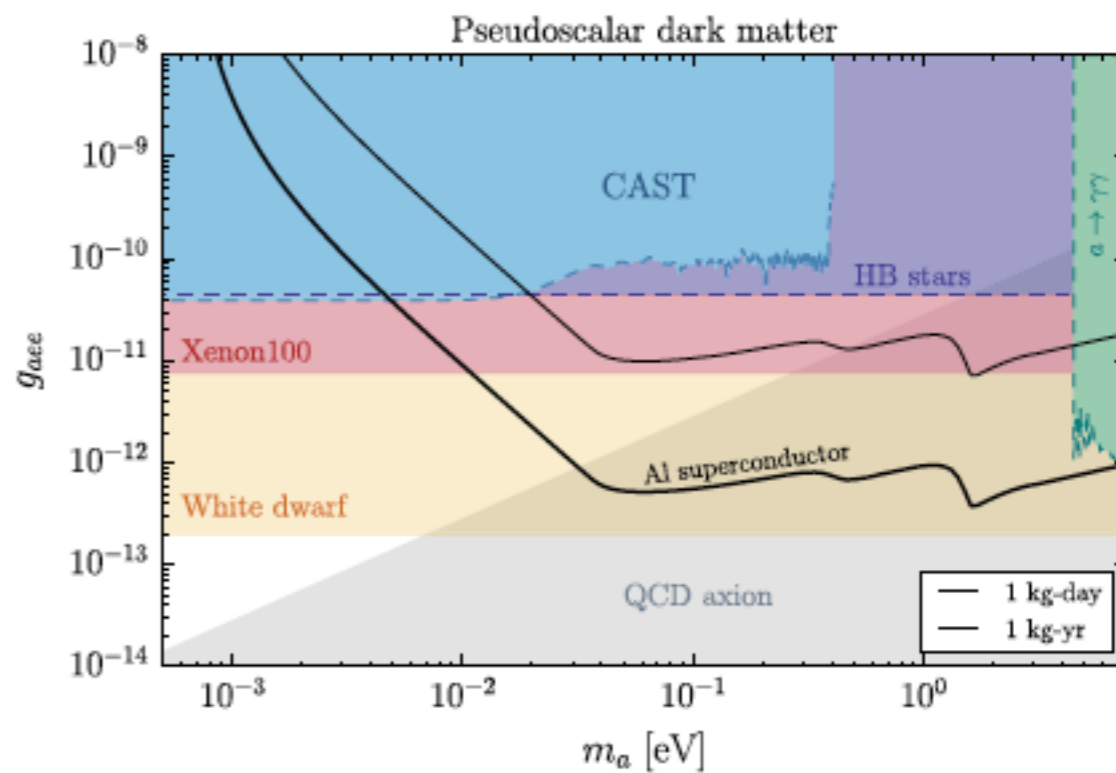
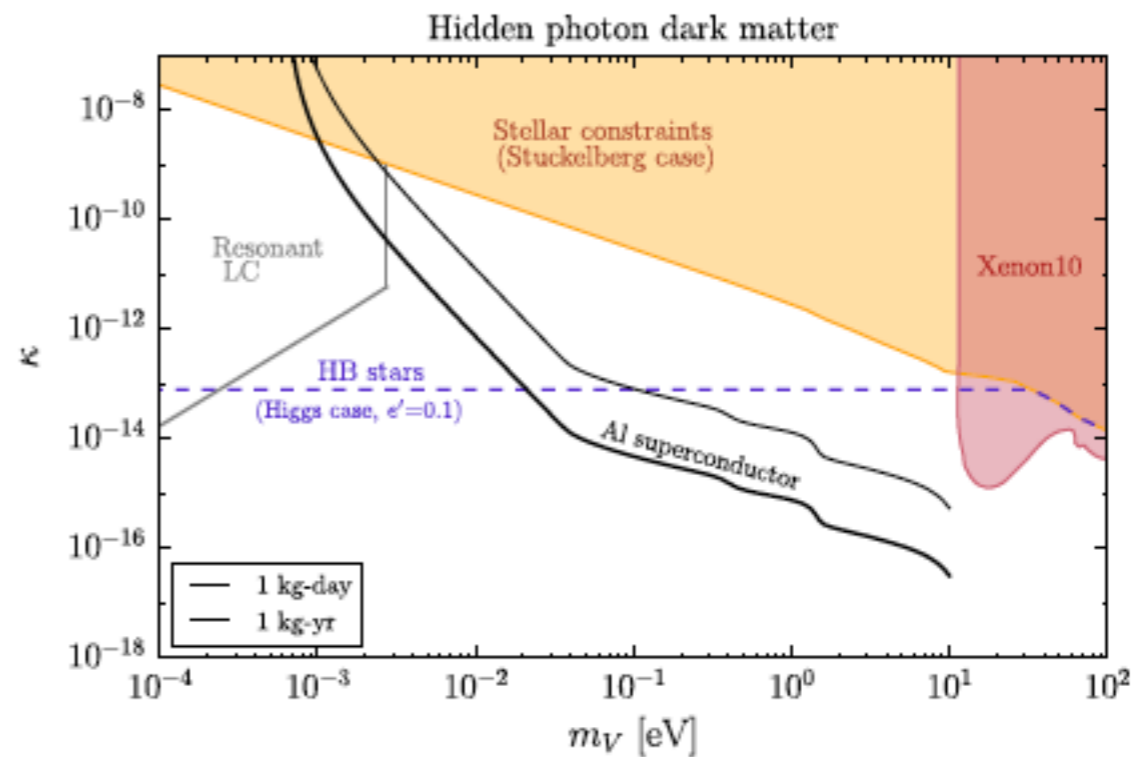


FIG. 1. Absorption process on electrons for an incoming relic particle X , where a phonon Φ is emitted in the final state: $X(q) + e(k) \rightarrow e(k') + \Phi(Q)$.



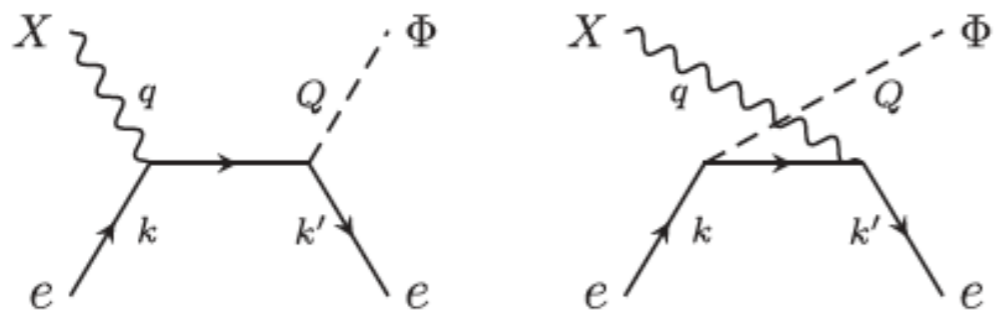
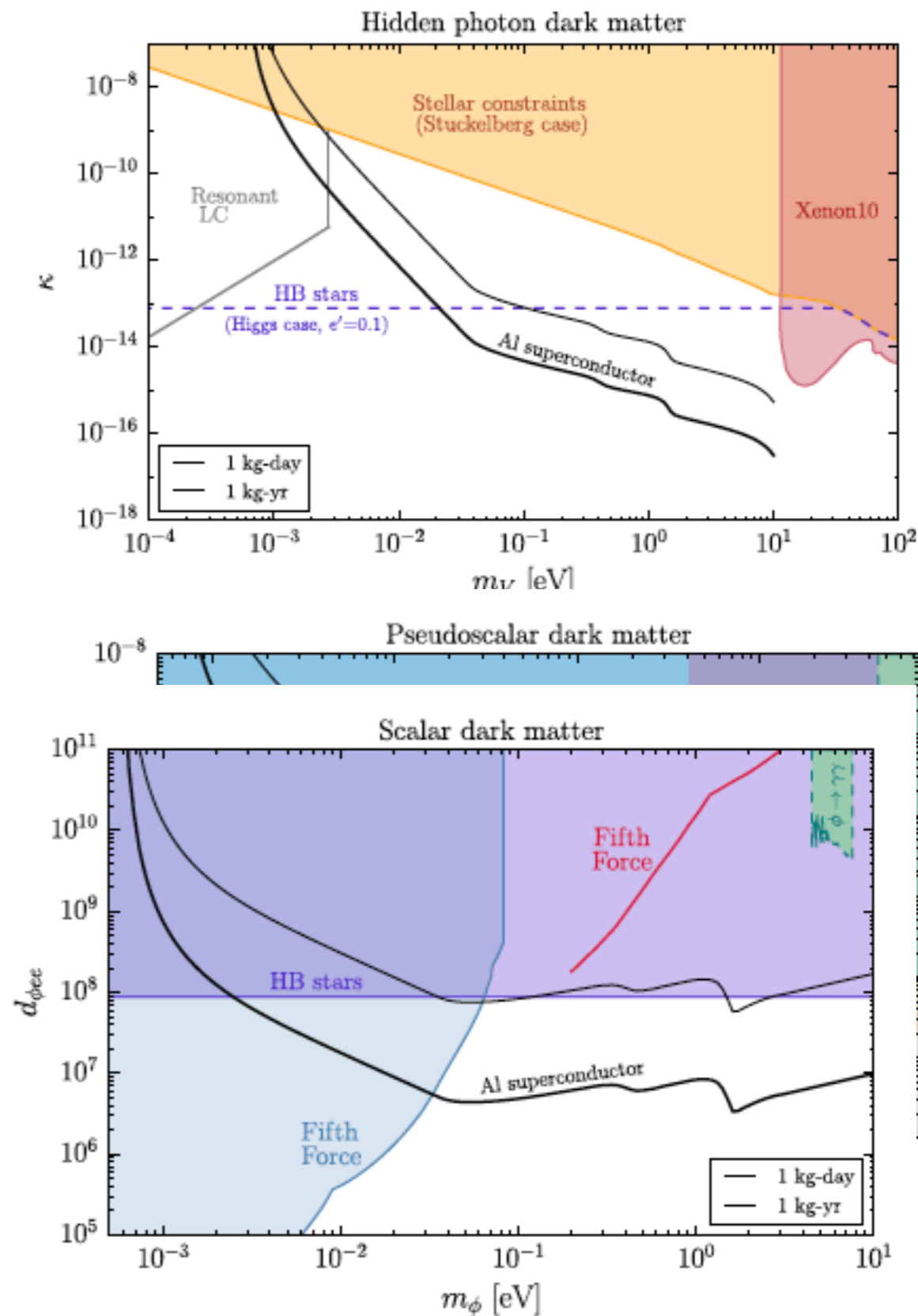
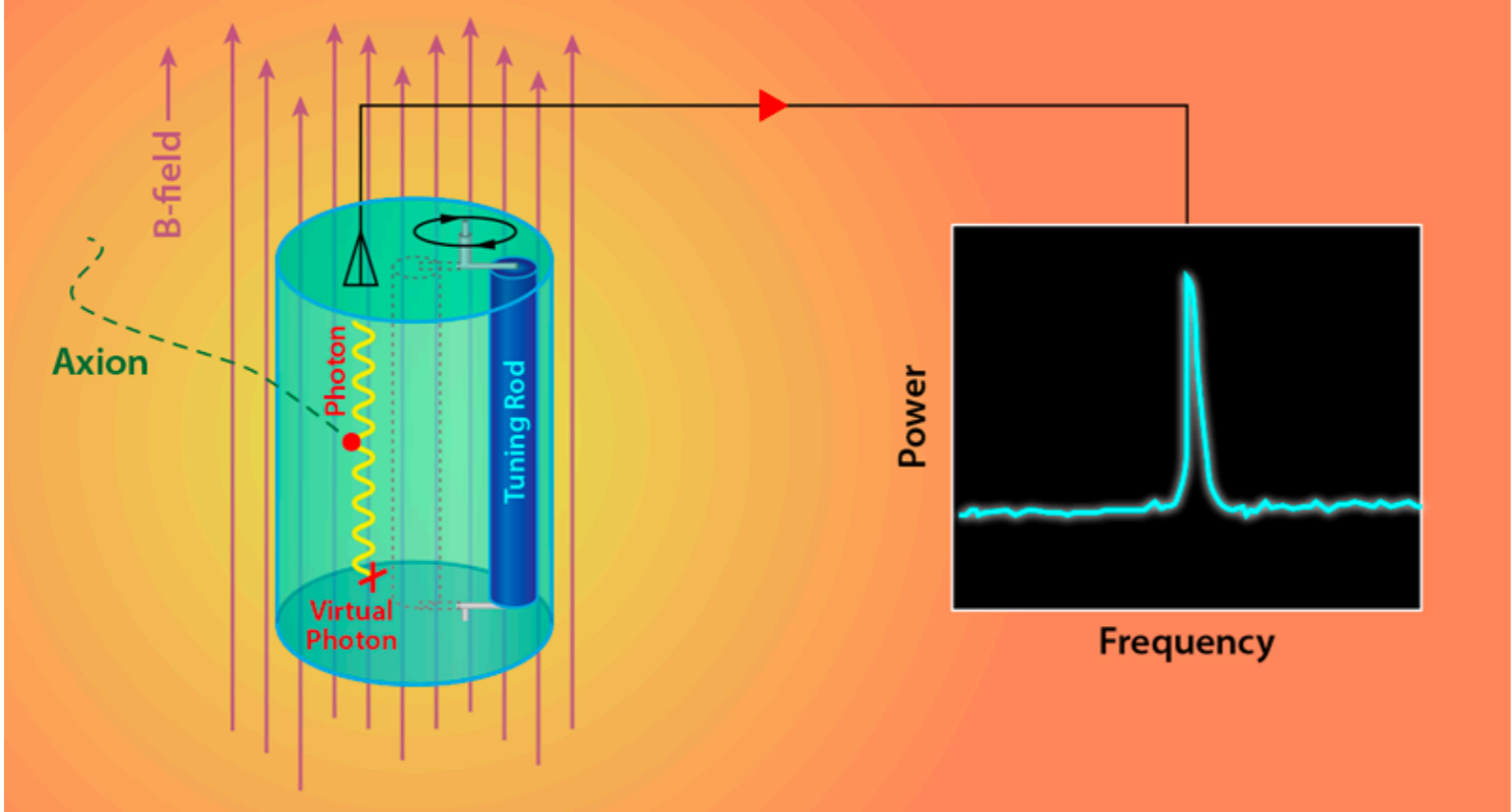
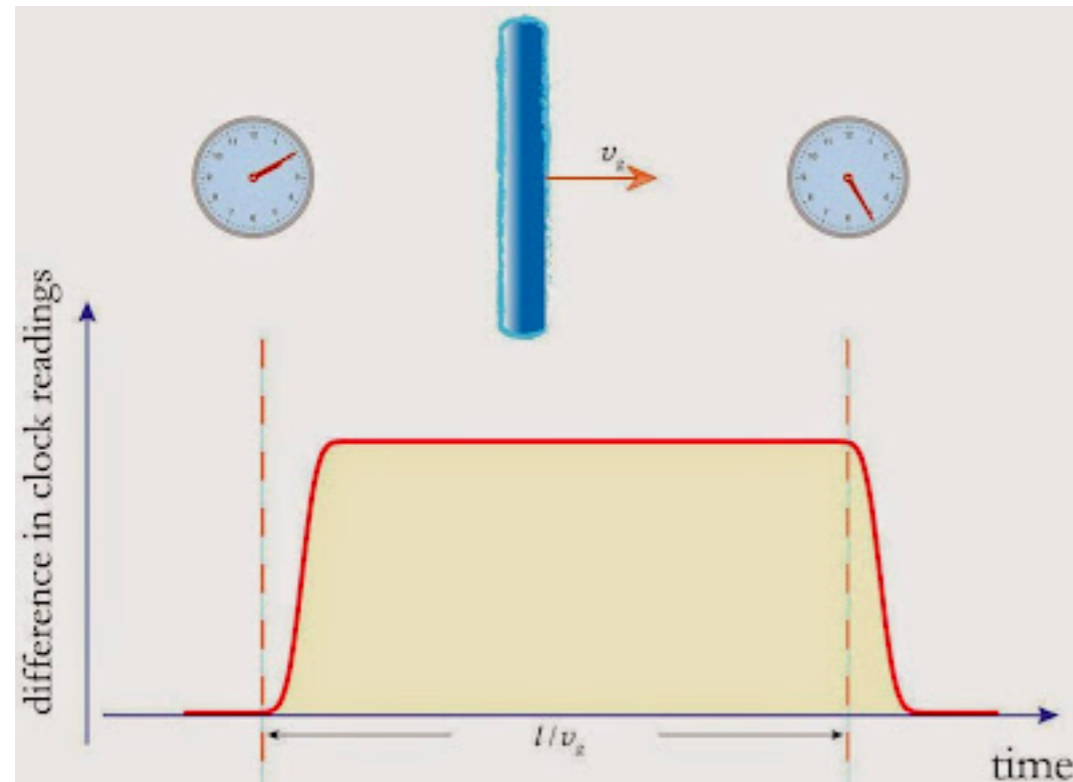


FIG. 1. Absorption process on electrons for an incoming relic particle X , where a phonon Φ is emitted in the final state: $X(q) + e(k) \rightarrow e(k') + \Phi(Q)$.

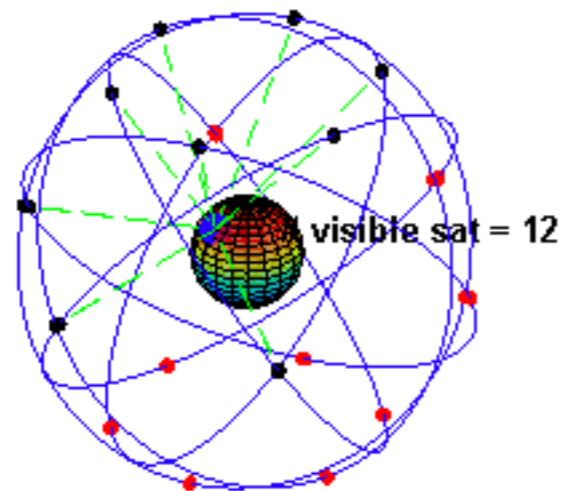


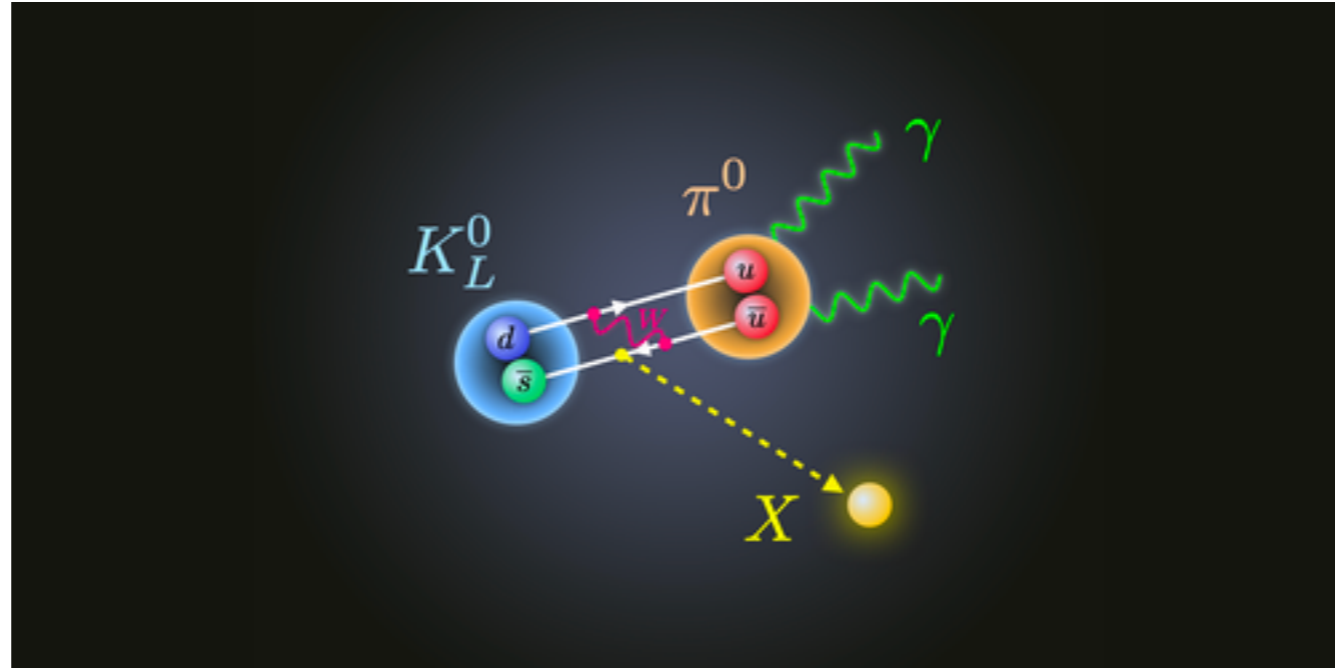




Derevianko and Pospelov calculated how long topological dark matter might de-synchronize a series of atomic clocks on GPS satellites -- essentially the window of time scientists would have to detect such a measurement.

They explain in a paper they published last November on the scientific paper repository [arXiv](https://arxiv.org/abs/1311.1244) (1311.1244) that the clocks would be desynchronized for about 180 seconds. Since atomic clocks are precise to within one nanosecond, they will need to be desynchronized by at least that amount in order for scientists to detect topological dark matter.





Спасибо за внимание!

